Relativistic quantum transport theory of hadronic matter: The coupled nucleon, Δ, and pion system

Guangjun Mao, L. Neise, H. Stöcker, and W. Greiner
Institut für Theoretische Physik der J. W. Goethe-Universität, Postfach 11 19 32, D-60054 Frankfurt am Main, Germany
(Received 23 March 1998)

We derive the relativistic quantum transport equation for the pion distribution function based on an effective Lagrangian of the QHD-II model. The closed-time-path Green's function technique and the semiclassical, quasiparticle, and Born approximations are employed in the derivation. Both the mean field and collision term are derived from the same Lagrangian and presented analytically. The dynamical equation for the pions is consistent with that for the nucleons and Δ's which we developed before. Thus, we obtain a relativistic transport model which describes the hadronic matter with N, Δ, and π degrees of freedom simultaneously. Within this approach, we investigate the medium effects on the pion dispersion relation as well as the pion absorption and pion production channels in cold nuclear matter. In contrast to the results of the nonrelativistic model, the pion dispersion relation becomes harder at low momenta and softer at high momenta as compared to the free one, which is mainly caused by the relativistic kinetics. The theoretically predicted free $\pi N \rightarrow \Delta$ cross section is in agreement with the experimental data. Medium effects on the $\pi N \rightarrow \Delta$ cross section and momentum-dependent Δ-decay width are shown to be substantial. [S0556-2813(99)00203-4]

PACS number(s): 24.10.Jv, 13.75.Cs, 21.65.+f, 25.75.−q

I. INTRODUCTION

Pion physics is an important topic in nuclear physics. Recently, it received renewed interest in relativistic heavy-ion collisions because pions are the most abundantly produced particles at relativistic energies. Studies of pionic many-body degrees of freedom in high-energy nucleus-nucleus collisions were initiated by Gyulassy and Greiner [1] and by Migdal [2]. Since then, considerable efforts from both experimental [3–9] and theoretical [10–26] groups were made to study various aspects of the in-medium pion dispersion relation and pion dynamics, such as the pion spectrum and pion and antipion flow in hot and dense nuclear matter. Because of the high interaction cross section of the pion with the nuclear environment, they are continuously absorbed by forming Δ resonances which then decay again into pions. Therefore, pions have a chance to be emitted during the whole course of the reaction. While the high-energy tail of the pion spectrum provides information about compressed and excited nuclear matter in the early reaction stage, the low-energy part of the pion spectrum and pion flow contain information of the in-medium pion potential and nuclear equation of state (EOS) [24,26]. The low- and high-energy pions originate from different stages of the collision. A detailed study of the pion dynamics allows to extract the time evolution of heavy-ion collisions.

On the other hand, dileptons produced from π^+-π^- annihilation [17,27–30] provide information on the high-density phase at time scales of 1 fm/c. Since dileptons can leave the reaction volume essentially undistorted by final-state interactions, as was first pointed out by Gale and Kapusta [27], they are expected to be a good tool for an investigation of the violent phases of high-energy heavy-ion collisions. Recent data by the CERES Collaboration [31] show a substantial modification of the dileptons yield which might be explained either by many-body effects [32] or by an enhanced ρ-meson production (via π^+-π^- annihilation) and a dropping ρ mass in the medium [33,34]. Indeed, the properties of the ρ meson as well as the Δ resonance are strongly influenced by the change of pion property in the medium due to the large $\rho \rightarrow \pi^+ \pi^-$ and $\Delta \rightarrow N\pi$ decay widths. A detailed knowledge of pion dynamics in heavy-ion collisions is a prerequisite for a quantitative description of dilepton production at SIS and SPS energies.

It was recently proposed that the difference between π^- and π^+ spectra can be attributed to the influence of isospin and Coulomb fields [35]. This should allow one to extract the effective Coulomb field at the instant of the average pion emission. Comparison of spectra of positively and negatively charged pions can also be used to learn about the freeze-out of the pions during the expansion phase [36,37]. It then provides a method to determine the size of fireball during the nuclear expansion process.

Since the importance of pions in heavy-ion collisions has been recognized for more than two decades, one may believe that elementary pion properties in the hot and dense nuclear matter are already well understood. Unfortunately, the situation is quite different from this expectation: understanding the pion dynamics in high-energy nucleus-nucleus collisions is still a major challenge to modern nuclear physics. This paradoxical circumstance seems to be mainly due to theoretical rather than experimental inadequacies. Experiments have been able to record the pion spectrum [6,8,38] and pion flow and antiflow [9,39] with rather high accuracy. A reasonably strict treatment of pions in the transport theories is, however, still not available. Most theoretical approaches included the interaction of the pions with the surrounding nuclear medium only by collision processes. A free-particle assumption was usually assigned to pions, while it is well known that the pion dispersion relation will be changed substantially in the medium due to the strong p-wave interaction. Some authors [21,22,26] implemented the real part of the pion optical po-

tential from the nonrelativistic Δ-hole model [40] to study the pion spectrum. In Ref. [26] a phenomenological parametrization suggested by Gale and Kapusta [27] was also tried. However, different model treatments gave rather different results. None of the currently available models are able to reproduce the experimental spectrum over the entire range of energy. The source of the problem seems to be that the observed quantities are sensitive to several of the unknown pion properties in the hot and dense matter. The most important ones are the in-medium pion dispersion relation (the real part of the pion self-energy) and the in-medium pion cross sections (the imaginary part of the pion self-energy). A self-consistent treatment of both the real part and imaginary part of the pion self-energy is necessary to obtain useful information from experimental observable. However, in transport theories one usually uses the experimentally determined free cross sections and incorporates a dispersion relation from the nonrelativistic Δ-hole model or simply employs the free-particle assumption. A self-consistent description of pions in transport models has not even been reached in the nonrelativistic case. In the present work, we still do not have a fully self-consistent treatment. But we go a step further than the present available relativistic transport theories; i.e., we derive the in-medium pion dispersion relation and the in-medium pion cross sections from the same Lagrangian and treat them in a relativistic description.

Another daunting obstacle to a quantitative description of pions in heavy-ion collisions is the width and shape of the Δ. As has been pointed out before, when a pion in the hot and dense matter collides with a nucleon, it will be absorbed to create a Δ. Then the Δ decays again into a pion-nucleon ''pair.'' Thus the amplitude for creating and absorbing pions will be sensitive to the in-medium Δ-decay width, which must be modified by the presence of matter due to the potential energies of N, Δ, and π. However, in the presently available transport models, the free Δ-decay width is commonly employed. From the theoretical point of view, realistic models for describing pions in dynamical processes should in principle at least also treat deltas and nucleons simultaneously in an unified framework.

It is the purpose of this paper to develop the relativistic transport theory for pions within the framework of the relativistic Vlasov-Uehling-Uhlenbeck (RVUU) and relativistic Boltzmann-Uchling-Uhlenbeck (RBUU) equation. The RVUU model has been applied successfully in studying of high-energy heavy-ion collisions [15,41–45]. In Ref. [15] we briefly discussed a possible extension to include the pion degree of freedom. By means of the density matrix method Wang *et al.* [46] developed a transport theory for the N, Δ, and π system. In their work pions are treated as a free particle; detailed expressions of the collision term are not given explicitly. On the other hand, in Refs. [47–53] we developed a set of self-consistent equations for N, Δ, and $N^*(1440)$ distribution functions in which both mean field and collision term are derived from the same effective Lagrangian and expressed analytically. However, mesons (σ,ω,π) were treated as virtual particles. In a physically reasonable scenario, the creation and destruction of real as well as virtual mesons ought to be described simultaneously and on the same self-consistent footing [54]. Hence, one is forced to solve coupled Boltzmann equations not only for baryons but also for all relevant mesons. This will cause significant numerical difficulties and might be beyond the ability of modern computers. As a first practical step, let us here treat the pions explicitly. The pion is the most frequently observed meson. The other mesons still remain treated as virtual mesons. This is the main strategy of our present work. Here we should note that the transport equations for σ and ω mesons were discussed in Refs. [15,55] based on the Walecka model [56]. In Ref. [55] the mesons turn out to be treated as free particles due to the approximations used in that work. Also, no concrete expressions for the collision term were given there. We will come back to this point in Sec. III.

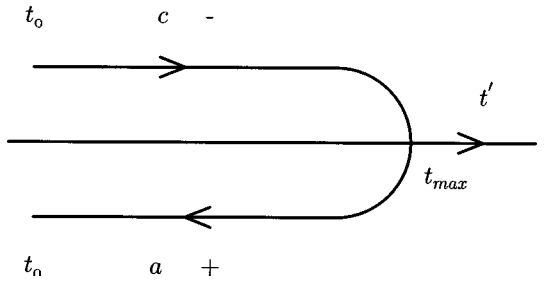

FIG. 1. Contour along the axis for an evaluation of the operator expectation value. In practice, t_0 is shifted to $-\infty$ and $t_{\max}$ to $+\infty$.

Starting from an effective Lagrangian of the QHD-II model [56] we here derive a RVUU equation for the pion distribution function in which both the mean field and the collision term are derived simultaneously and expressed analytically. In our framework a fully relativistic treatment is realized and medium effects are included. Furthermore, we treat N, Δ, and π in an unified framework based on the same effective Lagrangian and finally obtain a set of coupled equations for hadronic matter. The paper is organized as follows: In Sec. II we briefly review the closed-time-path Green's function technique which plays a central role in our derivation. An effective Lagrangian for the N, Δ, and π system interacting through the exchange of virtual mesons is also presented there. In Sec. III we derive the RVUU-type transport equation for the pion distribution function. The main ingredients of the equation are the relativistic mean field and collision terms, which are calculated from the same effective Lagrangian and presented analytically in Secs. IV and V, respectively. In Sec. VI we present the numerical results for the in-medium pion dispersion relation and Δ-formation cross section. Finally, a summary and outlook are given in Sec. VII.

II. PRELIMINARIES

In the present work we employ the closed-time-path Green's function technique. For a detailed description of this Green's function technique for nonequilibrium system, we refer to Refs. [57,58]. Here we give a brief review for the reader's convenience. In the Heisenberg picture the Green's function $G_F(1,2)$ of fermions and $\Delta_B(1,2)$ of bosons can be defined on the time contour depicted in Fig. 1 as

$$iG_F(1,2)\equiv\langle T[\Psi_H(1)\bar{\Psi}_H(2)]\rangle, \tag{1}$$

$$i\Delta_B(1,2)\equiv\langle T[\Phi_H(1)\Phi_H(2)]\rangle-\langle\Phi_H(1)\rangle\langle\Phi_H(2)\rangle, \tag{2}$$

where 1, 2 denote x_1, x_2; $\Psi_H(1)$ and $\bar{\Psi}_H(2)$ represent the field operators of the nucleon and delta in the Heisenberg picture and $\Phi_H(1)$ and $\Phi_H(2)$ are those of the σ, ω, π, and ρ. Here we have specified the initial state by assuming that its density operator commutes with the particle-number operator [57]. Furthermore, we assume that the initial state admits the Wick decomposition (is noncorrelated). Thus, in Eq. (1) the expectation value of a single fermionic field vanishes. In the case of bosonic Green's functions, the contributions from classical expectation values have been subtracted in order to concentrate on the field fluctuations around the classical values. On the other hand, the second term on the right-hand side of Eq. (2) explicitly indicates the presence of the *mean field*. According to the position of field operators on the time contour, we have four different Green's functions for fermions,

$$
\begin{aligned}
iG_F^{--}(1,2) &= \langle T^c \Psi_H(1) \bar{\Psi}_H(2) \rangle, \\
iG_F^{++}(1,2) &= \langle T^a \Psi_H(1) \bar{\Psi}_H(2) \rangle, \\
iG_F^{+-}(1,2) &= \langle \Psi_H(1) \bar{\Psi}_H(2) \rangle, \\
iG_F^{-+}(1,2) &= -\langle \bar{\Psi}_H(2) \Psi_H(1) \rangle,
\end{aligned} \tag{3}
$$

and four for bosons,

$$
\begin{aligned}
i\Delta_B^{--}(1,2) &= \langle T^c \Phi_H(1) \Phi_H(2) \rangle - \langle \Phi_H(1) \rangle \langle \Phi_H(2) \rangle, \\
i\Delta_B^{++}(1,2) &= \langle T^a \Phi_H(1) \Phi_H(2) \rangle - \langle \Phi_H(1) \rangle \langle \Phi_H(2) \rangle, \\
i\Delta_B^{+-}(1,2) &= \langle \Phi_H(1) \Phi_H(2) \rangle - \langle \Phi_H(1) \rangle \langle \Phi_H(2) \rangle, \\
i\Delta_B^{-+}(1,2) &= \langle \Phi_H(2) \Phi_H(1) \rangle - \langle \Phi_H(1) \rangle \langle \Phi_H(2) \rangle.
\end{aligned} \tag{4}
$$

Here T^c is the chronological ordering operator and T^a is the antichronological ordering operator. The designations $-$ and $+$ are attributed to the respective time path shown in Fig. 1.

We further on express the $G_F(1,2)$ and $\Delta_B(1,2)$ in a compact matrix form

$$
iG_F(1,2) = \begin{pmatrix} iG_F^{--}(1,2) & iG_F^{-+}(1,2) \\ iG_F^{+-}(1,2) & iG_F^{++}(1,2) \end{pmatrix} \tag{5}
$$

and

$$
i\Delta_B(1,2) = \begin{pmatrix} i\Delta_B^{--}(1,2) & i\Delta_B^{-+}(1,2) \\ i\Delta_B^{+-}(1,2) & i\Delta_B^{++}(1,2) \end{pmatrix}. \tag{6}
$$

It should be pointed out that the four Green's functions in Eq. (5) are not independent. They satisfy the following relations:

$$
iG_F^{--}(1,2) = \theta(t_1 - t_2) iG_F^{+-}(1,2) + \theta(t_2 - t_1) iG_F^{-+}(1,2), \tag{7}
$$

$$
iG_F^{++}(1,2) = \theta(t_1 - t_2) iG_F^{-+}(1,2) + \theta(t_2 - t_1) iG_F^{+-}(1,2). \tag{8}
$$

Here $\theta(t_1 - t_2)$ is defined as

$$
\theta(t_1 - t_2) = \begin{cases} 1, & t_1 \text{is later on a contour than } t_2, \\ 0, & t_1 \text{is earlier on a contour than } t_2. \end{cases} \tag{9}
$$

The same relations hold for the boson Green's functions in Eq. (6).

In order to use the powerful perturbation expansion method of field theory, we choose the interaction picture. The time-ordered products in Eqs. (1) and (2) can then be rewritten as

$$
\langle T[\Psi_H(1) \bar{\Psi}_H(2)] \rangle = \left\langle T\left[\exp\left(-i \int dx H_I(x) \right) \times \Psi_I(1) \bar{\Psi}_I(2) \right] \right\rangle, \tag{10}
$$

$$
\langle T[\Phi_H(1) \Phi_H(2)] \rangle = \left\langle T\left[\exp\left(-i \int dx H_I(x) \right) \times \Phi_I(1) \Phi_I(2) \right] \right\rangle, \tag{11}
$$

$$
\langle \Phi_H(1) \rangle = \left\langle T\left[\exp\left(-i \int dx H_I(x) \right) \Phi_I(1) \right] \right\rangle. \tag{12}
$$

Here $\psi_I(1), \bar{\psi}_I(2)$ and $\Phi_I(1), \Phi_I(2)$ represent the field operators in the interaction picture; $\int dx \equiv \int dt d\mathbf{x}$, $\int$ stands for an integral along the time axis given in Fig. 1. The definition of Eqs. (3) and (4) and the relations of Eqs. (7), (8) are still valid in the interaction picture for both the full Green's functions $G_F(1,2), \Delta_B(1,2)$ and zeroth-order Green's functions (i.e., noninteracting Green's functions) $G_F^0(1,2), \Delta_B^0(1,2)$. The detailed expressions of the zeroth-order Green's functions as well as H_I in Eqs. (10)–(12) are determined by the specific effective Lagrangian used in the model. As a preliminary step towards a complete description of hadronic matter, we first consider a system consisting of real nucleons, Δ's and pions interacting through the exchange of virtual σ, ω, π, and ρ mesons. In order to avoid extensive cancellations of large terms to correctly describe the small S-wave πN scattering length, we choose the phenomenological pseudovector form for the πNN and $\pi\Delta\Delta$ coupling. With this choice of coupling, the value of the S-wave πN scattering length turns out to be -0.010 [56] while the empirical value is -0.015 ± 0.015 [59]. The inclusion of the ρ-meson degree of freedom is important for the $\pi\pi$ scattering due to vector meson dominance [60]. We furthermore include two nonlinear meson coupling terms $\sigma\pi\pi$ and $\rho\pi\pi$ which are applied only to the $\pi\pi$ scattering. The total effective Lagrangian can then be written as

$$
\mathcal{L} = \mathcal{L}_F + \mathcal{L}_I. \tag{13}
$$

Here $\mathcal{L}_F$ is the Lagrangian density for free nucleon, Δ, and meson fields,

$$\mathcal{L}_{\mathrm{F}}=\bar{\psi}[i\gamma_\mu\partial^\mu-M_N]\psi+\bar{\psi}_{\Delta\nu}[i\gamma_\mu\partial^\mu-M_\Delta]\psi_\Delta^\nu+\frac{1}{2}\partial_\mu\sigma\partial^\mu\sigma$$
$$-U(\sigma)-\frac{1}{4}\omega_{\mu\nu}\omega^{\mu\nu}+U(\omega)+\frac{1}{2}(\partial_\mu\boldsymbol{\pi}\partial^\mu\boldsymbol{\pi}-m_\pi^2\boldsymbol{\pi}^2)$$
$$-\frac{1}{4}\boldsymbol{\rho}_{\mu\nu}\boldsymbol{\rho}^{\mu\nu}+\frac{1}{2}m_\rho^2\boldsymbol{\rho}_\mu\cdot\boldsymbol{\rho}^\mu, \tag{14}$$

and $U(\sigma),U(\omega)$ are the self-interaction part of the scalar field [61] and vector field [62,63],

$$U(\sigma)=\frac{1}{2}m_\sigma^2\sigma^2+\frac{1}{3}b(g_{NN}^\sigma\sigma)^3+\frac{1}{4}c(g_{NN}^\sigma\sigma)^4, \tag{15}$$

$$U(\omega)=\frac{1}{2}m_\omega^2\omega_\mu\omega^\mu\left(1+\frac{(\mathrm{g}_{NN}^\omega)^2}{2}\frac{\omega_\mu\omega^\mu}{Z^2}\right), \tag{16}$$

respectively. Here the field tensor for the rho and omega are given in terms of their potential fields by

$$\boldsymbol{\rho}_{\mu\nu}=\partial_\mu\boldsymbol{\rho}_\nu-\partial_\nu\boldsymbol{\rho}_\mu \tag{17}$$

and

$$\boldsymbol{\omega}_{\mu\nu}=\partial_\mu\boldsymbol{\omega}_\nu-\partial_\nu\boldsymbol{\omega}_\mu. \tag{18}$$

The interaction Lagrangian $\mathcal{L}_I$ consists of baryon-baryon, baryon-meson, and meson-meson terms, which are given by

$$\begin{aligned}\mathcal{L}_I&=\mathcal{L}_{NN}+\mathcal{L}_{\Delta\Delta}+\mathcal{L}_{\Delta N}+\mathcal{L}_{\sigma\pi}+\mathcal{L}_{\rho\pi}\\
&=g_{NN}^\sigma\bar{\psi}(x)\psi(x)\sigma(x)-g_{NN}^\omega\bar{\psi}(x)\gamma_\mu\psi(x)\omega^\mu(x)+g_{NN}^\pi\bar{\psi}(x)\gamma_\mu\gamma_5\boldsymbol{\tau}\cdot\psi(x)\partial^\mu\boldsymbol{\pi}(x)-\frac{1}{2}g_{NN}^\rho\bar{\psi}(x)\gamma_\mu\boldsymbol{\tau}\cdot\psi(x)\boldsymbol{\rho}^\mu(x)\\
&\quad+g_{\Delta\Delta}^\sigma\bar{\psi}_{\Delta\nu}(x)\psi_\Delta^\nu(x)\sigma(x)-g_{\Delta\Delta}^\omega\bar{\psi}_{\Delta\nu}(x)\gamma_\mu\psi_\Delta^\nu(x)\omega^\mu(x)+g_{\Delta\Delta}^\pi\bar{\psi}_{\Delta\nu}(x)\gamma_\mu\gamma_5\mathbf{T}\cdot\psi_\Delta^\nu(x)\partial^\mu\boldsymbol{\pi}(x)\\
&\quad-\frac{1}{2}g_{\Delta\Delta}^\rho\bar{\psi}_{\Delta\nu}(x)\gamma_\mu\mathbf{T}\cdot\psi_\Delta^\nu(x)\boldsymbol{\rho}^\mu(x)-g_{\Delta N}^\pi\bar{\psi}_{\Delta\mu}(x)\partial^\mu\boldsymbol{\pi}(x)\cdot\mathbf{S}^+\psi(x)-g_{\Delta N}^\pi\bar{\psi}(x)\mathbf{S}\psi_{\Delta\mu}(x)\cdot\partial^\mu\boldsymbol{\pi}(x)\\
&\quad+\frac{1}{2}g_{\sigma\pi}m_\sigma\sigma(x)\boldsymbol{\pi}(x)\cdot\boldsymbol{\pi}(x)+g_{\rho\pi}[\partial^\mu\boldsymbol{\pi}(x)\times\boldsymbol{\pi}(x)]\cdot\boldsymbol{\rho}_\mu(x)\\
&=g_{NN}^A\bar{\psi}(x)\Gamma_A^N\psi(x)\Phi_A(x)+g_{\Delta\Delta}^A\bar{\psi}_{\Delta\nu}(x)\Gamma_A^\Delta\psi_\Delta^\nu(x)\Phi_A(x)-g_{\Delta N}^\pi\bar{\psi}_{\Delta\mu}(x)\partial^\mu\boldsymbol{\pi}(x)\cdot\mathbf{S}^+\psi(x)\\
&\quad-g_{\Delta N}^\pi\bar{\psi}(x)\mathbf{S}\psi_{\Delta\mu}(x)\cdot\partial^\mu\boldsymbol{\pi}(x)+g_{\pi\pi}^A\pi_i(x)\Gamma_A^\pi\pi_j(x)\Phi_A(x).\end{aligned} \tag{19}$$

In the above expressions $\psi(x)$ is the Dirac spinor of the nucleon and $\psi_{\Delta\mu}(x)$ is the Rarita-Schwinger spinor of the Δ baryon. $\boldsymbol{\tau}$ is the isospin operator of the nucleon and $\mathbf{T}$ is the isospin operator of the Δ. Here $\mathbf{S}$ and $\mathbf{S}^+$ are the isospin transition operator between the isospin 1/2 and 3/2 fields. $g_{NN}^\pi=f_\pi/m_\pi, g_{\Delta N}^\pi=f^*/m_\pi; \Gamma_A^N=\gamma_A\tau_A, \Gamma_A^\Delta=\gamma_A T_A, \Gamma_A^\pi=\gamma_A^\pi\tau_A^\pi, A=\sigma,\omega,\pi,\rho$, the symbols and notation are given in Tables I and II for the baryon-baryon-meson vertex and meson interaction vertex, respectively.

The zeroth-order Green's functions of nucleons and Δ's as well as mesons corresponding to the free Lagrangian density of Eq. (14) are summarized in Appendix A, where the distribution functions of negative-energy states are neglected for fermions. They are kept for bosons. Considering that we will derive a transport equation for the pion in which we only treat the real pion with positive-energy states, we rewrite the zeroth-order Green's functions of the pion as

$$\Delta_\pi^{0\mp\mp}(x,k)=\frac{\pm1}{k^2-m_\pi^2\pm i\epsilon}-\frac{\pi i}{\omega(k)}\delta[k_0-\omega(k)]f_\pi(x,k), \tag{20}$$

$$\Delta_\pi^{0+-}(x,k)=-\frac{\pi i}{\omega(k)}\delta[k_0-\omega(k)][1+f_\pi(x,k)], \tag{21}$$

$$\Delta_\pi^{0-+}(x,k)=-\frac{\pi i}{\omega(k)}\delta[k_0-\omega(k)]f_\pi(x,k); \tag{22}$$

here $\omega(k)$ is the energy of the pion.

TABLE I. Symbols and notation used for the baryon-baryon-meson vertex; P_μ is the transformed four-momentum.

A	m_A	g_{NN}^A	$g_{\Delta\Delta}^A$	γ_A	τ_A	T_A	$\Phi_A(x)$	D_A^μ	D_A^i
σ	m_σ	g_{NN}^σ	$g_{\Delta\Delta}^\sigma$	1	1	1	$\sigma(x)$	1	1
ω	m_ω	$-g_{NN}^\omega$	$-g_{\Delta\Delta}^\omega$	γ_μ	1	1	$\omega^\mu(x)$	$-g^{\mu\nu}$	1
π	m_π	g_{NN}^π	$g_{\Delta\Delta}^\pi$	$\not{p}\gamma_5$	$\boldsymbol{\tau}$	$\mathbf{T}$	$\boldsymbol{\pi}$(x)	1	δ_{ij}
ρ	m_ρ	$-\frac{1}{2}g_{NN}^\rho$	$-\frac{1}{2}g_{\Delta\Delta}^\rho$	γ_μ	$\boldsymbol{\tau}$	$\mathbf{T}$	$\boldsymbol{\rho}^\mu(x)$	$-g^{\mu\nu}$	δ_{ij}

TABLE II. Symbols and notation used for the interaction vertex involving only mesons.

A	$g_{\pi\pi}^A$	γ_A^π	τ_A^π	$\Phi_A(x)$
σ	$\frac{1}{2}g_{\sigma\pi}m_\sigma$	1	δ_{ij}	$\sigma(x)$
ρ	$g_{\rho\pi}$	$i(p+q)_\mu$	ε_{ijk}	$\rho_k^\mu(x)$

III. DERIVATION OF THE QUANTUM TRANSPORT EQUATION FOR PIONS

A. Dyson equation and pion self-energy

With the discussions of Sec. II we can write down the pion Green's function in the interaction picture as

$$i\Delta_\pi(1,2)\delta_{ij}=\left\langle T\left[\exp\left(-i\oint dxH_I(x)\right)\boldsymbol{\pi}_I(1)\boldsymbol{\pi}_I(2)\right]\right\rangle - \left\langle T\left[\exp\left(-i\oint dxH_I(x)\right)\boldsymbol{\pi}_I(1)\right]\right\rangle \times\left\langle T\left[\exp\left(-i\oint dxH_I(x)\right)\boldsymbol{\pi}_I(2)\right]\right\rangle; \quad (23)$$

here $i, j=1, 2, 3$ represent the isospin indices of pion. In the following we suppress this subscript because at the end we will obtain a RVUU-type transport equation which is averaged on the isospin. Furthermore, the second term on the right-hand side of Eq. (23) vanishes in the spin- and isospin-saturated system. By expanding Eq. (23) perturbatively one can obtain the Dyson equation for the pion Green's function, which reads as

$$i\Delta_\pi(1,2)=i\Delta^0_\pi(1,2)+\oint dx_3\oint dx_4\Delta^0_\pi(1,4)\Pi(4,3)i\Delta_\pi(3,2); \quad (24)$$

here $\Pi(4,3)$ is the self-energy of the pion, which is also a matrix on the time contour:

$$\Pi(4,3)=\begin{pmatrix}\Pi^{--}(4,3) & \Pi^{-+}(4,3)\\ \Pi^{+-}(4,3) & \Pi^{++}(4,3)\end{pmatrix}. \quad (25)$$

Equation (24) is coupled to the Dyson equation of the nucleon [48,52],

$$iG(1,2)=iG^0(1,2)+\oint dx_3\oint dx_4G^0(1,4)\Sigma(4,3)iG(3,2), \quad (26)$$

and Δ [50],

$$iG_{\alpha\beta}(1,2)=iG^0_{\alpha\beta}(1,2) + \oint dx_3\oint dx_4G^0_{\alpha\nu}(1,4)\Sigma^{\nu\mu}(4,3)iG_{\mu\beta}(3,2), \quad (27)$$

through the self-energy terms of $\Pi(4,3)$, $\Sigma(4,3)$, and $\Sigma_{\nu\mu}(4,3)$. Here $G(1,2), G_{\alpha\beta}(1,2)$ are Green's functions of the nucleon and Δ, and $\Sigma(4,3), \Sigma_{\nu\mu}(4,3)$ are the respective self-energies. Equations (24), (26), and (27) are a set of dynamical equations for the hadronic matter. From Eqs. (26) and (27) we have derived the RVUU-type transport equations for the nucleon [15,47–49,52] and Δ [50,51] distribution functions. In this work we will develop a transport equation for the pion distribution function from Eq. (24), in which both the mean field and collision term will be expressed analytically. Since the lowest-order Feynman diagrams contributing to the two-body scattering cross sections are the Born diagrams, we consider the pion self-energy $\Pi(4,3)$ up to the *Born approximation*. In principle, one should calculate the in-medium cross sections and meson fields for all the particles within a relativistic *G*-matrix theory. However, since we have to deal with many reaction channels and many degrees of freedom, such calculations seem to be out of the present practical possibilities. For a qualitative insight in the cross sections and potentials we think that the Born approximation will be sufficient. A comparison between the cross sections for $\sigma^*_{NN\to NN}$ and $\sigma^*_{NN\to N\Delta}$ calculated in *G*-matrix theory [64,65] and in the Born approximation [47,48] shows differences only of the order of 10–20 %.

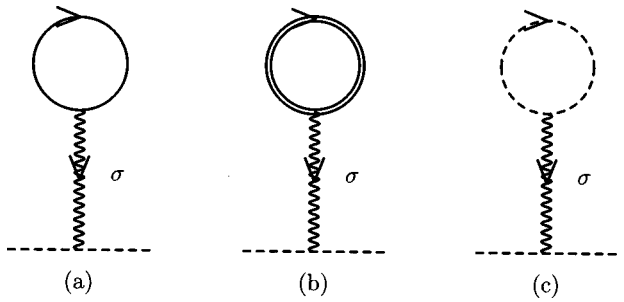

FIG. 2. Feynman diagrams contribute to the Hartree term of the pion self-energy. The wavy line denotes the exchanged virtual meson, the solid line, double line, and dashed line represent the nucleon, Δ, and pion, respectively.

The pion self-energy up to the Born term can be written as

$$\Pi(4,3)=\Pi_{\rm HF}(4,3)+\Pi_{\rm Born}(4,3); \quad (28)$$

here $\Pi_{\rm HF}(4,3)$ is the Hartree-Fock self-energy of the pion and $\Pi_{\rm Born}(4,3)$ is the Born self-energy. The corresponding Feynman diagrams are given in Figs. 2, 3, and 4.

In Fig. 3 we only take the baryon loops into account since the contributions of meson loops (σ-π and ρ-π mixed loop) are negligible [66] at zero temperature (finite temperatures are not taken into account explicitly in the present framework of microscopic transport theory). Furthermore, since the pseudovector form is chosen for the πNN and $\pi\Delta\Delta$ coupling, as discussed in Ref. [56] (Sec. 8.3), the contribution of the sigma-pion coupling term to the πN *S*-wave scattering lengths is small, of order $m_\pi^2/(M_N m_\sigma)$, and can be neglected; we drop the contribution of Fig. 2(a) and Fig. 2(b) to the pion self-energy. Therefore, only Fig. 2(c) contributes to the Hartree-term of the pion self-energy, which plays a role in the case that a large amount of pions are produced in relativistic heavy-ion collisions at very high energy. For the Born term we consider the Feynman diagrams contributing to the $\pi+N\to\pi+N$, $\pi+\Delta\to\pi+\Delta$, and $\pi+\pi\to\pi+\pi$ elastic scattering processes as depicted in Fig. 4. For the same reason we neglect the contribution of the σ exchange

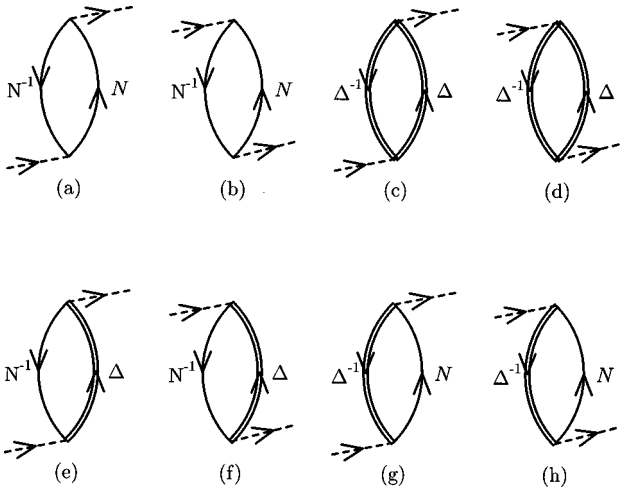

FIG. 3. Feynman diagrams contribute to the Fock term (one baryon loop) of the pion self-energy. Different lines denote the different particles as described in the caption of Fig. 2.

in Figs. 4(a) and 4(b). The Hartree-Fock self-energy $\Pi_{\rm HF}(4,3)$ and Born self-energy $\Pi_{\rm Born}(4,3)$ can then be expressed as

$$\Pi_{\rm HF}(4,3)=\Pi_H(4,3)+\Pi_{\rm loop}(4,3), \tag{29}$$

$$\Pi_{\rm loop}(4,3)=\Pi_{NN^{-1}}(4,3)+\Pi_{\Delta\Delta^{-1}}(4,3)+\Pi_{\Delta N^{-1}}(4,3)+\Pi_{N\Delta^{-1}}(4,3), \tag{30}$$

$$\Pi_{\rm Born}(4,3)=\Pi_a(4,3)+\Pi_b(4,3)+\Pi_c(4,3)+\Pi_d(4,3), \tag{31}$$

where the lower subscripts N^{-1} and Δ^{-1} in Eq. (30) denote the particles described by the nucleon and Δ distribution functions rather than the antiparticles which are not taken into account in this work because the gap between the effective masses of particles and antiparticles is much larger than the pion mass even at 3 times normal density (see Fig. 5). For even higher densities and temperatures the production of particle and antiparticle pairs becomes more important and the anti-particle degree of freedom should be taken into account. The lower subscripts *a*, *b*, *c*, *d* in Eq. (31) denote the terms contributed from Figs. 4(a)–4(d), respectively. $\Pi_{\Delta\Delta^{-1}}(4,3)$ [corresponding to Figs. 3(c) and 3(d)] and $\Pi_{N\Delta^{-1}}(4,3)$ [corresponding to Figs. 3(g) and 3(h)] are usually neglected in the investigation of the influence of the in-medium pion dispersion relation on the pion dynamics in relativistic heavy-ion collisions [16,17,21,22,26]. However, it was recently reported that more than 30% of nucleons are excited to the resonance states, especially the Δ resonance, in Au+Au collisions at an incident energy of 2 GeV/nucleon [67]. That means that the contributions of Figs. 3(c), 3(d) and 3(g), 3(h) should be taken into account once the problem of the in-medium pion dispersion relation is concerned in *relativistic heavy-ion collisions*. To our knowledge, up to now no investigation of this has been made in transport theories. Here we note that this effect has been addressed in some nonrelativistic calculations of the pion self-energy in static nuclear matter at finite temperature [68].

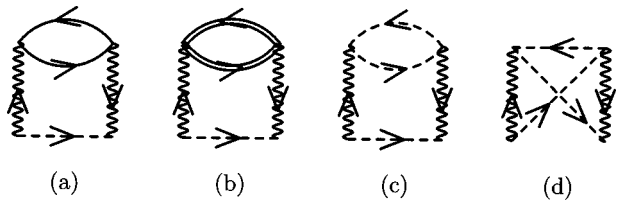

FIG. 4. Feynman diagrams contribute to the Born term of the pion self-energy. Different lines denote the different particles as described in the caption of Fig. 2. The imaginary part of (a) contributes to the $\pi N\to\pi N$ elastic cross section, and (b) to the $\pi\Delta\to\pi\Delta$, (c),(d) to the $\pi\pi\to\pi\pi$ elastic cross section, respectively.

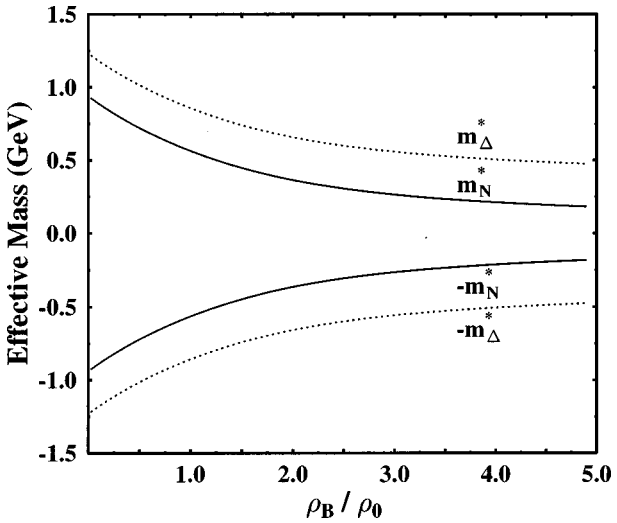

FIG. 5. The gap between the effective masses of particles and antiparticles as a function of density. Universal coupling strengths for the nucleons and Δ's are assumed.

The concrete expressions of self-energies in Eqs. (29)–(31) can be written down according to the standard Feynman rules:

$$\Pi_H(4,3)=\frac{3}{4}(g_{\sigma\pi}m_\sigma)^2\delta(3,4)\int dx_3'\Delta_\pi^0(3',3')i\Delta_\sigma^0(3',4), \tag{32}$$

$$\Pi_{NN^{-1}}(4,3)=-2i(g_{NN}^\pi)^2{\rm tr}[\not P\gamma_5 G^0(3,4)\not P\gamma_5 G^0(4,3)], \tag{33}$$

$$\Pi_{\Delta\Delta^{-1}}(4,3)=-5i(g_{\Delta\Delta}^\pi)^2{\rm tr}[\not P\gamma_5 G^0_{\mu\nu}(3,4)\not P\gamma_5 G^{0,\nu\mu}(4,3)], \tag{34}$$

$$\Pi_{\Delta N^{-1}}(4,3)=\frac{4}{3}i(g_{\Delta N}^\pi)^2{\rm tr}[G^0(3,4)P^\mu P^\nu G^0_{\nu\mu}(4,3)], \tag{35}$$

$$\Pi_{N\Delta^{-1}}(4,3)=\frac{4}{3}i(g_{\Delta N}^\pi)^2{\rm tr}[P^\mu P^\nu G^0_{\mu\nu}(3,4)G^0(4,3)], \tag{36}$$

$$\Pi_a(4,3)=\sum_{r_4 t_5 t_6}\int dx_5\int dx_6\langle r|g^{\rho}_{\pi\pi}\Gamma^{\pi}_{\rho}|r_4\rangle\Delta^0_{\pi}(4,3)\langle r_4|g^{\rho}_{\pi\pi}\Gamma^{\pi}_{\rho}|r\rangle \mathrm{tr}\{\langle t_6|g^{\rho}_{NN}\Gamma^{N}_{\rho}|t_5\rangle G^0(5,6)$$
$$\times\langle t_5|g^{\rho}_{NN}\Gamma^{N}_{\rho}|t_6\rangle G^0(6,5)\}\Delta^0_{\rho}(4,6)\Delta^0_{\rho}(5,3)D_{\rho}D_{\rho}, \tag{37}$$

$$\Pi_b(4,3)=\sum_{r_4 T_5 T_6}\int dx_5\int dx_6\langle r|g^{\rho}_{\pi\pi}\Gamma^{\pi}_{\rho}|r_4\rangle\Delta^0_{\pi}(4,3)\langle r_4|g^{\rho}_{\pi\pi}\Gamma^{\pi}_{\rho}|r\rangle \mathrm{tr}\{\langle T_6|g^{\rho}_{\Delta\Delta}\Gamma^{\Delta}_{\rho}|T_5\rangle G^{0,\sigma\rho}(5,6)$$
$$\times\langle T_5|g^{\rho}_{\Delta\Delta}\Gamma^{\Delta}_{\rho}|T_6\rangle G^0_{\rho\sigma}(6,5)\}\Delta^0_{\rho}(4,6)\Delta^0_{\rho}(5,3)D_{\rho}D_{\rho}, \tag{38}$$

$$\Pi_c(4,3)=-\sum_{r_4 r_5 r_6}\int dx_5\int dx_6\langle r|g^{A}_{\pi\pi}\Gamma^{\pi}_{A}|r_4\rangle\Delta^0_{\pi}(4,3)\langle r_4|g^{A}_{\pi\pi}\Gamma^{\pi}_{A}|r\rangle\langle r_6|g^{A}_{\pi\pi}\Gamma^{\pi}_{A}|r_5\rangle\Delta^0_{\pi}(5,6)$$
$$\times\langle r_5|g^{A}_{\pi\pi}\Gamma^{\pi}_{A}|r_6\rangle\Delta^0_{\pi}(6,5)\Delta^0_{A}(4,6)\Delta^0_{A}(5,3)D_{A}D_{A}, \tag{39}$$

$$\Pi_d(4,3)=-\sum_{r_4 r_5 r_6}\int dx_5\int dx_6\langle r|g^{A}_{\pi\pi}\Gamma^{\pi}_{A}|r_4\rangle\Delta^0_{\pi}(4,5)\langle r_4|g^{B}_{\pi\pi}\Gamma^{\pi}_{B}|r_5\rangle\Delta^0_{\pi}(5,6)\langle r_5|g^{A}_{\pi\pi}\Gamma^{\pi}_{A}|r_6\rangle\Delta^0_{\pi}(6,3)$$
$$\times\langle r_6|g^{B}_{\pi\pi}\Gamma^{\pi}_{B}|r\rangle\Delta^0_{A}(4,6)\Delta^0_{B}(5,3)D_{A}D_{B}. \tag{40}$$

In Eqs. (37)–(40), A, $B=\sigma,\rho;r,r_4,r_5,r_6$ represent the isospin of pions, t_5,t_6 denote the isospin of nucleons and T_5,T_6 of Δ's. The definition of the symbols is given in Tables I and II. The transformed four-momentum P_{μ} in Eqs. (33)–(36) stems from the derivative coupling of the baryon-baryon-pion vertex used in our calculations.

B. Kadanoff-Baym equation

Introducing the differential operator of the Klein-Gordon field

$$\hat{\Delta}^{-1}_{01}=\partial^1_{\mu}\partial^{\mu}_1+m^2_{\pi} \tag{41}$$

and applying it to the both sides of Eq. (24), with the help of relation [69]

$$\hat{\Delta}^{-1}_{01}\Delta^0_{\pi}(1,2)=-\delta(1,2), \tag{42}$$

we obtain

$$\hat{\Delta}^{-1}_{01}i\Delta_{\pi}(1,2)=-i\delta(1,2)-\int dx_3\Pi(1,3)i\Delta_{\pi}(3,2). \tag{43}$$

It has been shown in Sec. II that only two components of $\Delta_{\pi}(1,2)$ are independent, from which the dynamical equations for the distribution function and the spectral function can be constituted [70]. Since we will use the *quasiparticle approximation* in the derivation, the spectral function turns out to be a δ function on the mass shell. Thus, in the present work it will be sufficient to consider only one component of $\Delta_{\pi}(1,2)$, i.e., $\Delta^{-+}_{\pi}(1,2)$, which is directly related to the single-particle density matrix in the case of $t_1=t_2$ [57]. The equation of motion for $\Delta^{-+}_{\pi}(1,2)$ can be extracted from Eq. (43). Before doing it, let us firstly look at the Feynman diagrams in Figs. 2, 3, and 4 which will be taken into account under Born approximation.

As is well known, the RVUU-type transport equation contains two important ingredients, i.e., the transport part related to the real part of the pion self-energy and the collision term corresponding to the imaginary part. The Hartree term of Fig. 2(c) only contributes to the real part. However, the loop diagrams in Fig. 3 and the Born diagrams in Fig. 4 include both real and imaginary parts. It should be pointed out that the baryon lines in Fig. 3 denoted by the symbols N or Δ represent virtual baryons (nucleon or delta) when one calculates the real part of the self-energies. They are not on-shell particles. The corresponding terms for the σ and ω self-energies are neglected in the derivation of Ref. [55] for the σ and ω transport equations because they used the restriction that all Green's functions in the Feynman diagrams should be on the mass shell. Consequently, mesons (σ and ω) became free particles in their framework. To our opinion, in computing the real part of self-energies, which mainly relates to the virtual processes, it is not necessary to keep all particles on the mass shell which will essentially give the imaginary part. It is well known that the particle-hole excitation is very important for the in-medium pion dispersion relation which will certainly have influence on the pion spectra and pion flow in relativistic heavy-ion collisions [26] and should be taken into account in any realistic transport models for pions. For the imaginary part of the self-energies from one-loop diagrams in Fig. 3, we include only the contributions of Figs. 3(e) and 3(h), which contribute to the important Δ-formation process of $N+\pi\rightarrow\Delta$ and Δ-decay process of $\Delta\rightarrow N+\pi$, respectively. The reason is as follows: the contributions of the imaginary part of Figs. 3(a)–3(d), in which both the baryon lines are on the mass shell, correspond to the process that a nucleon (Δ) decays into a nucleon (Δ) and a pion, which is forbidden due to energy-momentum conservation (here we do not consider the Cherenkov radiation discussed in Ref. [71]; this process might be possible at high densities where the pion has a spacelike four-momentum due to its large potential); Figs. 3(f) and 3(g) do not correspond

to realistic physical processes when the pion has a positive energy. Since the matrix elements are the same for both Δ-formation and Δ-decay processes, we only need to calculate the imaginary part of Fig. 3(e) explicitly. In view of the Born diagrams we take only the imaginary parts into account and drop all the real parts which in principle are the corrections to the real part of the Hartree-Fock self-energies. The imaginary part of the self-energies can be expressed by $\Pi^{\pm\mp}_{\rm coll}(1,3)$, which is defined as

$$\Pi^{\pm\mp}_{\rm coll}(1,3)=\Pi^{\pm\mp}_{\rm Born}(1,3)+\Pi^{\pm\mp}_{3(e)}(1,3); \tag{44}$$

here $\Pi^{\pm\mp}_{3(e)}(1,3)$ represents the imaginary part of Fig. 3(e). The equation of motion for $\Delta^{-+}_{\pi}(1,2)$ can then be written as

$$\begin{aligned}[\partial^1_\mu\partial^\mu_1+m^2_\pi+\Pi_H(1)]i\Delta^{-+}_\pi(1,2)=&-\int_{t_0}^{t}dx_3[\mathrm{Re}\,\Pi^{--}_{\rm loop}(1,3)]i\Delta^{-+}_\pi(3,2)-\int_{t}^{t_0}dx_3\Pi^{-+}_{\rm coll}(1,3)i[\mathrm{Re}\,\Delta^{++}_\pi(3,2)]\\&-\int_{t_0}^{t_1}dx_3[\Pi^{+-}_{\rm coll}(1,3)-\Pi^{-+}_{\rm coll}(1,3)]i\Delta^{-+}_\pi(3,2)+\int_{t_0}^{t_2}dx_3\Pi^{-+}_{\rm coll}(1,3)\\&\times[i\Delta^{+-}_\pi(3,2)-i\Delta^{-+}_\pi(3,2)].\end{aligned} \tag{45}$$

Equation (45) is the so-called Kadanoff-Baym equation [72]. Here the symbol ''Re'' denotes the real part of the corresponding self-energies. The second term on the right-hand side of Eq. (45) corresponds to the spreading width in the spectral function. It should be dropped under the quasiparticle approximation [70] which will be introduced later. The structure of the third and fourth terms on the right-hand side of Eq. (45) implies that they contribute to the collision term of the transport equation. The concrete expressions of the self-energies read as

$$\Pi_H(1)=\frac{3}{4}(g_{\sigma\pi}m_\sigma)^2\left\{\int_{t_0}^{t}dx'_3\Delta^{0--}_\pi(3',3')i\Delta^{0--}_\sigma(3',1)+\int_{t}^{t_0}dx'_3\Delta^{0++}_\pi(3',3')i\Delta^{0+-}_\sigma(3',1)\right\}, \tag{46}$$

$$\Pi^{--}_{NN^{-1}}(1,3)=-2i(g^\pi_{NN})^2\mathrm{tr}[\not P\gamma_5G^{0--}(3,1)\not P\gamma_5G^{0--}(1,3)], \tag{47}$$

$$\Pi^{--}_{\Delta\Delta^{-1}}(1,3)=-5i(g^\pi_{\Delta\Delta})^2\mathrm{tr}[\not P\gamma_5G^{0--}_{\mu\nu}(3,1)\not P\gamma_5G^{0--,\nu\mu}(1,3)], \tag{48}$$

$$\Pi^{--}_{\Delta N^{-1}}(1,3)=\frac{4}{3}i(g^\pi_{\Delta N})^2\mathrm{tr}[G^{0--}(3,1)P^\mu P^\nu G^{0--}_{\nu\mu}(1,3)], \tag{49}$$

$$\Pi^{--}_{N\Delta^{-1}}(1,3)=\frac{4}{3}i(g^\pi_{\Delta N})^2\mathrm{tr}[P^\mu P^\nu G^{0--}_{\mu\nu}(3,1)G^{0--}(1,3)], \tag{50}$$

$$\Pi^{\pm\mp}_{3(e)}(1,3)=\frac{4}{3}i(g^\pi_{\Delta N})^2\mathrm{tr}[G^{0\mp\pm}(3,1)P^\mu P^\nu G^{0\pm\mp}_{\nu\mu}(1,3)]. \tag{51}$$

The expressions of the Born terms are rather complicated. If one does not write out the isospin factor explicitly, $\Pi^{\pm\mp}_a(1,3)$ can be expressed as

$$\begin{aligned}\Pi^{\pm\mp}_a(1,3)\sim&\int_{t_0}^{t}dx_5\int_{t_0}^{t}dx_6\Delta^{0\pm\mp}_\pi(1,3)\{\mathrm{tr}[G^{0\mp\mp}(5,6)G^{0\mp\mp}(6,5)]\Delta^{0\pm\mp}_A(1,6)\Delta^{0\mp\mp}_A(5,3)\\&+\mathrm{tr}[G^{0\pm\pm}(5,6)G^{0\pm\pm}(6,5)]\Delta^{0\pm\pm}_A(1,6)\Delta^{0\pm\mp}_A(5,3)-\mathrm{tr}[G^{0\mp\pm}(5,6)G^{0\pm\mp}(6,5)]\Delta^{0\pm\pm}_A(1,6)\Delta^{0\mp\mp}_A(5,3)\\&-\mathrm{tr}[G^{0\pm\mp}(5,6)G^{0\mp\pm}(6,5)]\Delta^{0\pm\mp}_A(1,6)\Delta^{0\pm\mp}_A(5,3)\}.\end{aligned} \tag{52}$$

Other Born terms can be written down in the same way.

C. RVUU equation of the pion

Defining $X=\frac{1}{2}(x_1+x_2), y=x_1-x_2, x'=x_3-x_2$, and taking the Wigner transformation on the both sides of Eq. (45), we arrive at

$$\left[\frac{1}{4}\partial_\mu^X\partial_X^\mu - iP^\mu\partial_\mu^X - P^2 + m_\pi^2 + \Pi_H(X) + \mathrm{Re}\,\Pi_{\mathrm{loop}}^{--}(X,P) - \frac{i}{2}\partial_X^\mu\Pi_H(X)\partial_\mu^P + \frac{i}{2}\partial_P^\mu\,\mathrm{Re}\,\Pi_{\mathrm{loop}}^{--}(X,P)\partial_\mu^X - \frac{i}{2}\partial_X^\mu\,\mathrm{Re}\,\Pi_{\mathrm{loop}}^{--}(X,P)\partial_\mu^P\right]$$

$$\times i\Delta_\pi^{-+}(X,P) = -\int dy e^{iPy}\int_{-\infty}^{\tau} dx'[\Pi_{\mathrm{coll}}^{+-}(y-x',X)i\Delta_\pi^{-+}(x',X) - \Pi_{\mathrm{coll}}^{-+}(y-x',X)i\Delta_\pi^{+-}(x',X)]. \quad (53)$$

Here we have adopted the *semiclassical approximation*, in which the Green's functions and self-energies are assumed to be peaked around the relative coordinate and smoothly changing with the center-of-mass coordinate. The details of the Wigner transformation are given in Appendix B. The Hermitian conjugate equation of Eq. (53) reads as

$$\left[\frac{1}{4}\partial_\mu^X\partial_X^\mu + iP^\mu\partial_\mu^X - P^2 + m_\pi^2 + \Pi_H(X) + \mathrm{Re}\,\Pi_{\mathrm{loop}}^{--}(X,P) + \frac{i}{2}\partial_X^\mu\Pi_H(X)\partial_\mu^P - \frac{i}{2}\partial_P^\mu\,\mathrm{Re}\,\Pi_{\mathrm{loop}}^{--}(X,P)\partial_\mu^X + \frac{i}{2}\partial_X^\mu\,\mathrm{Re}\,\Pi_{\mathrm{loop}}^{--}(X,P)\partial_\mu^P\right]$$

$$\times i\Delta_\pi^{-+}(X,P) = -\int dy e^{iPy}\int_{\tau}^{\infty} dx'[\Pi_{\mathrm{coll}}^{-+}(y-x',X)i\Delta_\pi^{+-}(x',X) - \Pi_{\mathrm{coll}}^{+-}(y-x',X)i\Delta_\pi^{-+}(x',X)]. \quad (54)$$

We drop the term of $\partial_X^\mu\partial_\mu^X$ in Eqs. (53) and (54) since it may be viewed as of higher order than the other terms within the *gradient expansion* used in the Wigner transformation. If one would keep this term, the pion Green's function could be nonzero for off-shell four-momenta [73]. In this paper we only consider real on-shell pions. The summation of Eqs. (53) and (54) gives

$$[P^2 - m_\pi^2 - \Pi_H(X) - \mathrm{Re}\,\Pi_{\mathrm{loop}}^{--}(X,P)]i\Delta_\pi^{-+}(X,P) = 0, \quad (55)$$

and the subtraction of them yields

$$\left\{P^\mu\partial_\mu^X + \frac{1}{2}\partial_X^\mu\Pi_H(X)\partial_\mu^P + \frac{1}{2}\partial_X^\mu\,\mathrm{Re}\,\Pi_{\mathrm{loop}}^{--}(X,P)\partial_\mu^P - \frac{1}{2}\partial_P^\mu\,\mathrm{Re}\,\Pi_{\mathrm{loop}}^{--}(X,P)\partial_\mu^X\right\}i\Delta_\pi^{-+}(X,P)$$

$$= \frac{1}{2}[\Pi_{\mathrm{coll}}^{+-}(X,P)\Delta_\pi^{-+}(X,P) - \Pi_{\mathrm{coll}}^{-+}(X,P)\Delta_\pi^{+-}(X,P)]. \quad (56)$$

Now we introduce the *quasiparticle approximation* and dress the masses and momenta in the zeroth-order Green's functions appearing in the self-energies with the effective masses and momenta. The canonical variables X, P are then transformed to the kinetic variables x, p which will be used in the RVUU code for the simulation of relativistic heavy-ion collisions. Since the pion is a pseudoscalar particle, we have $P_\mu = p_\mu$. Medium effects are included through the effective mass which is defined as

$$m_\pi^{*2}(x,p) = m_\pi^2 + \Pi_H(x) + \mathrm{Re}\,\Pi_{\mathrm{loop}}^{--}(x,p). \quad (57)$$

The on-shell condition is guaranteed by Eq. (55):

$$p_0^2 - \omega^{*2}(p) = 0; \quad (58)$$

here

$$\omega^*(p) = [\mathbf{p}^2 + m_\pi^{*2}(x,p)]^{1/2}. \quad (59)$$

We further define a distribution function

$$i\Delta_\pi^{-+}(x,p) = \frac{\pi}{\omega^*(p)}Z_B\delta[p^0 - \omega^*(p)]f_\pi(\mathbf{x},\mathbf{p},\tau), \quad (60)$$

where

$$Z_B^{-1} = 1 - \frac{1}{2\omega^*(p)}\left.\frac{\partial\,\mathrm{Re}\,\Pi_{\mathrm{loop}}^{--}(x,p)}{\partial p_0}\right|_{p_0=\omega^*(p)}. \quad (61)$$

In the following we drop the derivative term in Eq. (61) since it will cause significant difficulty in deriving the collision term. In the nuclear medium the quantum numbers of the pion can be either transported as a physical pion or as a Δ-hole bound state. In several studies of the nonrelativistic Δ-hole model one considers the mixing between these two branches of the pion dispersion relation [21,22,26]. In this case strength is redistributed between the two branches as a function of momentum. Therefore, the wave function renormalization factor is essential and in principle it can be calculated from the energy dependence of the pion self-energy. However, in practical applications in transport theories only phenomenological simulations of this mixing have been investigated, Since we neglect the Δ-hole branch in our relativistic dynamical treatment, we put $Z_B^{-1} = 1$. This does not cause any difficulty with the conservation laws as can be seen from Eq. (F3). We simply obtain a different but still conserved current. An improvement over this not very satisfactory situation might be achieved if one studies relativistic transport theories beyond the quasiparticle approximation [70]. Especially, the inclusion of bound states in transport theory has been, however, studied only in a very few nonrelativistic cases near equilibrium up to now, e.g., for the formation of deutron in nuclear matter [74]. It is clear that the

relativistic bound-state problem is much more involved than the nonrelativistic one. Therefore, we neglect this problem here. Through inserting Eq. (60) into Eq. (56) one obtains the self-consistent RVUU equation for the pion distribution function:

$$\left\{ p^\mu \partial_\mu^x + \frac{1}{2}\partial_x^\mu \Pi_H(x)\partial_\mu^p + \frac{1}{2}\partial_x^\mu \,\mathrm{Re}\,\Pi_{\mathrm{loop}}^{--}(x,p)\partial_\mu^p - \frac{1}{2}\partial_p^\mu \,\mathrm{Re}\,\Pi_{\mathrm{loop}}^{--}(x,p)\partial_\mu^x \right\} \frac{f_\pi(\mathbf{x},\mathbf{p},\tau)}{\omega^*(p)} = F_c(x,p). \tag{62}$$

In Appendix F we show that this equation satisfies the conservation laws of the current and energy-momentum tensor. The left-hand side of Eq. (62) is the transport part and the right-hand side is the collision term, which includes two parts,

$$F_c(x,p) = F_{N\pi\to\Delta}(x,p) + F_{\mathrm{el}}(x,p)\,, \tag{63}$$

stemming from the $N\pi\to\Delta$ process and π-hadron elastic scattering processes, respectively. Other reactions are not included in the present work. The collision term can be further expressed via in-medium differential cross sections (Sec. V).

IV. CALCULATION OF THE MEAN FIELD

In Sec. III we derived the RVUU-type transport equation for the pion distribution function. The left-hand side of the equation is the transport part and the right-hand side is the collision term. The heart of the equation is the mean field, which relates to the in-medium pion dispersion relation, and the π-relevant in-medium differential cross sections. In this section and the next section we will evaluate concrete expressions of them. Before coming to it, we would like to emphasize again that in the present work we consider only the π meson as a real meson. σ,ω, and ρ mesons are still viewed as virtual ones. In other words, the terms relating to the distribution functions of σ,ω, and ρ mesons vanish. After Wigner transformation, Eqs. (46)–(50) turn out to be

$$\Pi_H(x) = \frac{3}{4}(g_{\sigma\pi}m_\sigma)^2 \int \frac{d^4q}{(2\pi)^4} \Delta_\pi^{0--}(x,q) i \Delta_\sigma^{0--}(x,0), \tag{64}$$

$$\Pi_{NN^{-1}}^{--}(x,p) = -2i(g_{NN}^\pi)^2 \int \frac{d^4q}{(2\pi)^4} \times \mathrm{tr}[\not p \gamma_5 G^{0--}(x,q) \not p \gamma_5 G^{0--}(x,p+q)], \tag{65}$$

$$\Pi_{\Delta\Delta^{-1}}^{--}(x,p) = -5i(g_{\Delta\Delta}^\pi)^2 \int \frac{d^4q}{(2\pi)^4} \times \mathrm{tr}[\not p \gamma_5 G_{\mu\nu}^{0--}(x,q) \not p \gamma_5 G^{0--,\nu\mu}(x,p+q)], \tag{66}$$

$$\Pi_{\Delta N^{-1}}^{--}(x,p) = \frac{4}{3} i (g_{\Delta N}^\pi)^2 \int \frac{d^4q}{(2\pi)^4} \mathrm{tr}[G^{0--}(x,q) p^\mu p^\nu G_{\nu\mu}^{0--} \times (x,p+q)], \tag{67}$$

$$\Pi_{N\Delta^{-1}}^{--}(x,p) = \frac{4}{3} i (g_{\Delta N}^\pi)^2 \int \frac{d^4q}{(2\pi)^4} \mathrm{tr}[p^\mu p^\nu G_{\mu\nu}^{0--}(x,q) G^{0--} \times (x,p+q)]. \tag{68}$$

In the next step we insert the zeroth-order Green's functions for baryons (Appendix A) and pions [Eqs. (20)–(22)] into Eqs. (64)–(68) to obtain concrete expressions of the real part of the pion self-energies. Several approximations are made here. First, we take the quasiparticle approximation in which the free masses and momenta in the zeroth-order Green's functions are addressed by the effective masses and momenta. Second, the first term on the right-hand side of Eq. (20), which will appear in Eq. (64) in the calculation of the Hartree term, is dropped as usually done according to the *physical* arguments (otherwise, it will cause divergence) [75]. Third, in computing Eqs. (65)–(68), we drop the contributions of antiparticles contained in the baryon Green's functions of $G^{0--}(x,q)$ and $G_{\mu\nu}^{0--}(x,q)$. The zeroth-order Green's functions used in this section then read as

$$\Delta_\sigma^{0--}(x,q) = \frac{1}{q^2 - m_\sigma^2 + i\epsilon}, \tag{69}$$

$$\Delta_\pi^{0--}(x,q) = -\frac{\pi i}{\omega^*(q)} \delta[q_0 - \omega^*(q)] f_\pi(\mathbf{x},\mathbf{q},\tau), \tag{70}$$

$$G^{0--}(x,q) = \frac{\not q + m^*}{2E^*(q)} \left[\frac{1}{q_0 - E^*(q) + i\epsilon} + 2\pi i \delta[q_0 - E^*(q)] f(\mathbf{x},\mathbf{q},\tau) \right], \tag{71}$$

$$G_{\mu\nu}^{0--}(x,q) = \frac{\not q + m_\Delta^*}{2E_\Delta^*(q)} D_{\mu\nu}(q) \left[\frac{1}{q_0 - E_\Delta^*(q) + i\epsilon} + 2\pi i \delta[q_0 - E_\Delta^*(q)] f_\Delta(\mathbf{x},\mathbf{q},\tau) \right], \tag{72}$$

where $E^*(q) = [\mathbf{q}^2 + m^{*2}]^{1/2}$, $E_\Delta^*(q) = [\mathbf{q}^2 + m_\Delta^{*2}]^{1/2}$, and $D_{\mu\nu}(q)$ is given in Appendix A. The definition of m^* and m_Δ^* will be given later. It is interesting to notice that only the Green's functions on the upper branch of the time contour, which are similar to the ones used in the standard effective field theory, enter in the calculations.

The Hartree term can be directly worked out,

$$\Pi_H(x) = -\frac{1}{4}(g_{\sigma\pi})^2 \rho_S(\pi); \tag{73}$$

here $\rho_S(\pi)$ is the scalar density of pions:

$$\rho_S(\pi)=\frac{3}{2(2\pi)^3}\int d\mathbf{q}\frac{1}{\sqrt{\mathbf{q}^2+m_\pi^{*2}}}f_\pi(\mathbf{x},\mathbf{q},\tau). \tag{74}$$

For the one-loop diagrams we have to distinguish the real and virtual baryons. The first terms on the right-hand side of Eqs. (71) and (72) describe the virtual nucleon and delta, which are denoted by the N and Δ in the Feynman diagrams in Fig. 3. The second terms with distribution functions represent the real nucleon and delta, and denoted by the N^{-1} and Δ^{-1} on the Feynman diagrams. Through inserting Eqs. (71) and (72) into Eqs. (65)–(68), after some straightforward algebra we obtain the real part of the self-energies:

$$\mathrm{Re}\,\Pi^{--}_{NN^{-1}}(x,p)$$
$$=-2(g^\pi_{NN})^2\int\frac{d^3q}{(2\pi)^3}\left[\frac{A(p,q)}{4E^*(q)E^*(p+q)}\times\frac{f(\mathbf{x},\mathbf{q},\tau)}{E^*(p+q)-E^*(q)-p_0}+p_0\to-p_0\right], \tag{75}$$

$$\mathrm{Re}\,\Pi^{--}_{\Delta\Delta^{-1}}(x,p)$$
$$=-5(g^\pi_{\Delta\Delta})^2\int\frac{d^3q}{(2\pi)^3}\left[\frac{B(p,q)}{4E^*_\Delta(q)E^*_\Delta(p+q)}\times\frac{f_\Delta(\mathbf{x},\mathbf{q},\tau)}{E^*_\Delta(p+q)-E^*_\Delta(q)-p_0}+p_0\to-p_0\right], \tag{76}$$

$$\mathrm{Re}\,\Pi^{--}_{\Delta N^{-1}}(x,p)$$
$$=\frac{4}{3}(g^\pi_{\Delta N})^2\int\frac{d^3q}{(2\pi)^3}\left[\frac{C(p,q)}{4E^*(q)E^*_\Delta(p+q)}\times\frac{f(\mathbf{x},\mathbf{q},\tau)}{E^*_\Delta(p+q)-E^*(q)-p_0}+p_0\to-p_0\right], \tag{77}$$

$$\mathrm{Re}\,\Pi^{--}_{N\Delta^{-1}}(x,p)$$
$$=\frac{4}{3}(g^\pi_{\Delta N})^2\int\frac{d^3q}{(2\pi)^3}\left[\frac{D(p,q)}{4E^*_\Delta(q)E^*(p+q)}\times\frac{f_\Delta(\mathbf{x},\mathbf{q},\tau)}{E^*(p+q)-E^*_\Delta(q)-p_0}+p_0\to-p_0\right]; \tag{78}$$

here,

$$A(p,q)=4[p_\mu^2(p\cdot q)_A-2m^{*2}p_\mu^2+2(p\cdot q)_A^2], \tag{79}$$

$$(p.q)_A=\frac{1}{2}\{[E^*(q)+p_0]^2-E^{*2}(p+q)-p_\mu^2\}, \tag{80}$$

$$B(p,q)=-\frac{8}{9m_\Delta^{*4}}\{2p_\mu^4m_\Delta^{*2}[(p\cdot q)_B-m_\Delta^{*2}]-2p_\mu^2(p\cdot q)_B^2[(p.q)_B-3m_\Delta^{*2}]-5p_\mu^2m_\Delta^{*4}\times[(p\cdot q)_B-2m_\Delta^{*2}]-2(p\cdot q)_B^2[2(p\cdot q)_B^2+2(p\cdot q)_Bm_\Delta^{*2}+5m_\Delta^{*4}]\}, \tag{81}$$

$$(p.q)_B=\frac{1}{2}\{[E^*_\Delta(q)+p_0]^2-E^{*2}_\Delta(p+q)-p_\mu^2\}, \tag{82}$$

$$C(p,q)=-\frac{8}{3m_\Delta^{*2}}[p_\mu^4+2p_\mu^2(p\cdot q)_C-m_\Delta^{*2}p_\mu^2+(p\cdot q)_C^2]\times[(p\cdot q)_C+m^{*2}+m^*m^*_\Delta], \tag{83}$$

$$(p.q)_C=\frac{1}{2}\{[E^*(q)+p_0]^2-E^{*2}_\Delta(p+q)+m^{*2}_\Delta-m^{*2}-p_\mu^2\}, \tag{84}$$

$$D(p,q)=\frac{8}{3m_\Delta^{*2}}[m_\Delta^{*2}p_\mu^2-(p\cdot q)_D^2]\times[(p\cdot q)_D+m^*m^*_\Delta+m^{*2}_\Delta], \tag{85}$$

$$(p.q)_D=\frac{1}{2}\{[E^*_\Delta(q)+p_0]^2-E^{*2}(p+q)+m^{*2}-m^{*2}_\Delta-p_\mu^2\}. \tag{86}$$

Here we already dropped the contributions from virtual particle-particle excitations (which are divergent), in consistent with the mean field approximation. Otherwise, one has to renormalize it which may be difficult in many situations. The effective mass of pion is defined in Eq. (57). The effective masses and momenta of nucleon and Δ are defined as [48,50,52,53]

$$m^*(x)=M_N-g^\sigma_{NN}\sigma(x), \tag{87}$$

$$m^*_\Delta(x)=M_\Delta-g^\sigma_{\Delta\Delta}\sigma(x), \tag{88}$$

$$p^\mu_N(x)=P^\mu_N-g^\omega_{NN}\omega^\mu(x), \tag{89}$$

$$p^\mu_\Delta(x)=P^\mu_\Delta-g^\omega_{\Delta\Delta}\omega^\mu(x). \tag{90}$$

The mean fields of $\sigma(x)$ and $\omega^\mu(x)$ are obtained through the following field equations within the *local density approximation:*

$$m_\sigma^2\sigma(x)+b(g^\sigma_{NN})^3\sigma^2(x)+c(g^\sigma_{NN})^4\sigma^3(x)=g^\sigma_{NN}\rho_S(N)+g^\sigma_{\Delta\Delta}\rho_S(\Delta)+\frac{1}{2}g_{\sigma\pi}m_\sigma\rho_S(\pi), \tag{91}$$

$$m_\omega^2\omega^\mu(x)+\frac{(g^\omega_{NN})^2m_\omega^2}{Z^2}[\omega^\mu(x)]^3=g^\omega_{NN}\rho^\mu_V(N)+g^\omega_{\Delta\Delta}\rho^\mu_V(\Delta). \tag{92}$$

The scalar and vector densities of the nucleon and Δ are defined as

$$\rho_S(i)=\frac{\gamma(i)}{(2\pi)^3}\int d\mathbf{q}\frac{m_i^*}{\sqrt{\mathbf{q}^2+m_i^{*2}}}f_i(\mathbf{x},\mathbf{q},\tau), \tag{93}$$

$$\rho_V^\mu(i)=\frac{\gamma(i)}{(2\pi)^3}\int d\mathbf{q}\frac{q^\mu}{\sqrt{\mathbf{q}^2+m_i^{*2}}}f_i(\mathbf{x},\mathbf{q},\tau). \tag{94}$$

The abbreviations $i=N,\Delta$, and $\gamma(i)=4$, 16, correspond to the nucleon and delta, respectively.

In Eqs. (87)–(90) we have dropped the Fock term of the nucleon and Δ self-energies since it makes only a small contribution. The Feynman diagrams for the Hartree term of nucleon and Δ self-energies can be drawn in the same way as in Fig. 2 by replacing the pion external line with the nucleon and Δ line. One may notice that the main contributions to the mean field of the nucleon and Δ come from the Hartree term while to the pion from the Fock term (one-loop diagrams). The situation is caused by the pseudovector coupling for the pion adopted in our considerations. If one uses pseudoscalar coupling for πNN and $\pi\Delta\Delta$ vertex, the pion will have a scalar self-energy from the Hartree term similar to the nucleon's and Δ's. But this term turns out to be so large that the effective mass of the pion will become almost 5 times more massive at the normal density of nuclear matter than in the vacuum [66]. This may not be a realistic case.

V. CALCULATION OF THE COLLISION TERM

A. In-medium $N\pi\rightarrow\Delta$ cross section and Δ-decay width

Now we come to calculate the right-hand side of Eq. (62), i.e., the collision term. The part corresponding to the Δ-formation cross section reads as

$$\begin{aligned}F_{N\pi\rightarrow\Delta}(x,p)&=\frac{1}{2}[\Pi_{3(e)}^{+-}(x,p)\Delta_\pi^{-+}(x,p)-\Pi_{3(e)}^{-+}(x,p)\Delta_\pi^{+-}(x,p)]\\&=\int\frac{d^3q}{(2\pi)^3}\int\frac{d^3k}{(2\pi)^3}(2\pi)^4\delta^{(4)}(p+q-k)\\&\quad\times W(p,q,k)(F_2^0-F_1^0);\end{aligned} \tag{95}$$

here F_2^0,F_1^0 are the Nordheim-Uehling-Uhlenbeck factors of the gain (F_2^0) and loss (F_1^0) terms:

$$F_2^0=[1+f_\pi(\mathbf{x},\mathbf{p},\tau)][1-f(\mathbf{x},\mathbf{q},\tau)]f_\Delta(\mathbf{x},\mathbf{k},\tau), \tag{96}$$

$$F_1^0=f_\pi(\mathbf{x},\mathbf{p},\tau)f(\mathbf{x},\mathbf{q},\tau)[1-f_\Delta(\mathbf{x},\mathbf{k},\tau)]. \tag{97}$$

$W(p,q,k)$ is the transition probability of the $N\pi\rightarrow\Delta$ process:

$$\begin{aligned}W(p,q,k)&=-\frac{(g_{\Delta N}^\pi)^2}{6\omega^*(p)E^*(q)E_\Delta^*(k)}\mathrm{tr}[(\not q+m^*)p^\mu p^\nu\\&\quad\times(\not k+m_\Delta^*)D_{\nu\mu}(k)]\\&=\frac{(g_{\Delta N}^\pi)^2}{\omega^*(p)E^*(q)E_\Delta^*(k)}\frac{1}{18m_\Delta^{*2}}[(m_\Delta^*+m^*)^2\\&\quad-m_\pi^{*2}]^2[(m^*-m_\Delta^*)^2-m_\pi^{*2}].\end{aligned} \tag{98}$$

In working out the second equality of Eq. (98) we have used the relations $k=p+q$ and $p\cdot q=(m_\Delta^{*2}-m^{*2}-m_\pi^{*2})/2$ from the energy-momentum conservation and on-shell conditions.

In the above derivation all baryons are treated as elementary particles as usually done in quantum field theory. However, the Δ is a resonance that can decay. A mass distribution function of the Breit-Wigner form is commonly introduced to describe the resonances with broadwidths [19,76]. However, one mostly discusses the problem in free space. Here we assume that the same form of distribution function applies to the medium with free quantities replaced by effective quantities. That is, we introduce a Breit-Wigner function for the Δ resonance in the medium,

$$F(m_\Delta^{*2})=\frac{1}{\pi}\frac{m_0^*\Gamma^*(|\mathbf{p}|)}{(m_\Delta^{*2}-m_0^{*2})^2+m_0^{*2}\Gamma^{*2}(|\mathbf{p}|)}, \tag{99}$$

where $\Gamma^*(|\mathbf{p}|)$ is the in-medium momentum-dependent Δ-decay width. $\mathbf{p}$ is the relative momentum between nucleon and pion in the Δ-rest system:

$$\mathbf{p}^2=\frac{[m_\Delta^{*2}-(m^*+m_\pi^*)^2][m_\Delta^{*2}-(m^*-m_\pi^*)^2]}{4m_\Delta^{*2}}. \tag{100}$$

m_0^* is defined by Eq. (88) with the free Δ mass M_Δ replaced by its resonance mass M_0. Inserting the mass-distribution function of Eq. (99) into Eq. (95), we have

$$\begin{aligned}F_{N\pi\rightarrow\Delta}(x,p)&=\int\frac{d^3q}{(2\pi)^3}\int\frac{d^3k}{(2\pi)^3}\int dm_\Delta^{*2}(2\pi)^4\delta^{(4)}\\&\quad\times(p+q-k)W(p,q,k)F(m_\Delta^{*2})(F_2^0-F_1^0)\\&=\int\frac{d^3q}{(2\pi)^3}v\sigma_{\mathrm{abs}}(s)(F_2^0-F_1^0).\end{aligned} \tag{101}$$

In the second line of the above equation we already expressed the collision term with the cross section [77]. Since we are now in the Δ-rest system, the effective total energy of the system s equals the effective Δ mass m_Δ^*. Here $\sigma_{\mathrm{abs}}(m_\Delta^*)$ reads as

$$\begin{aligned}\sigma_{\mathrm{abs}}(m_\Delta^*)&=\frac{2\pi}{|\mathbf{p}|}\frac{(g_{\Delta N}^\pi)^2}{9m_\Delta^{*3}}[(m_\Delta^*+m^*)^2-m_\pi^{*2}]^2\\&\quad\times[(m^*-m_\Delta^*)^2-m_\pi^{*2}]F(m_\Delta^{*2}).\end{aligned} \tag{102}$$

Performing an average over the initial states and writing out $F(m_\Delta^{*2})$ explicitly, we arrive at the cross section of the $N\pi\rightarrow\Delta$ process:

$$\sigma^*_{N\pi\to\Delta}(m^*_\Delta)=\frac{(g^\pi_{\Delta N})^2}{18m^{*3}_\Delta|\mathbf{p}|}[(m^*_\Delta+m^*)^2-m^{*2}_\pi]^2\times[(m^*-m^*_\Delta)^2-m^{*2}_\pi]\times\frac{m^*_0\Gamma^*(|\mathbf{p}|)}{(m^{*2}_\Delta-m^{*2}_0)^2+m^{*2}_0\Gamma^{*2}(|\mathbf{p}|)}. \tag{103}$$

According to Ref. [78], the resonant cross section can also be expressed by means of the decay width:

$$\sigma^*_{N\pi\to\Delta}=\frac{4\pi}{|\mathbf{p}|^2}\frac{(2J+1)}{(2s+1)}\frac{(2I+1)}{(2t+1)(2r+1)}\times\frac{m^{*2}_0\Gamma^{*2}(|\mathbf{p}|)}{(m^{*2}_\Delta-m^{*2}_0)^2+m^{*2}_0\Gamma^{*2}(|\mathbf{p}|)}; \tag{104}$$

here I, J are the isospin and spin of the Δ; t,s are that of the nucleon; and r is the isospin of the pion. Comparing Eqs. (103) and (104) we obtain the in-medium Δ-decay width, which reads as

$$\Gamma^*(|\mathbf{p}|)=\frac{|\mathbf{p}|}{16\pi m^*_0}\frac{(g^\pi_{\Delta N})^2}{6m^{*3}_\Delta}[(m^*_\Delta+m^*)^2-m^{*2}_\pi]^2\times[(m^*-m^*_\Delta)^2-m^{*2}_\pi]. \tag{105}$$

In this way, we give a clear-cut relation between in-medium Δ-decay width and Δ-formation cross section.

B. Elastic pion-hadron scattering

In this subsection we derive analytical expressions for calculating the in-medium $\pi+N\to\pi+N$, $\pi+\Delta\to\pi+\Delta$, and $\pi+\pi\to\pi+\pi$ elastic scattering cross sections. The corresponding part of the collision term can be written as

$$F_{\rm el}(x,p)=\frac{1}{2}[\Pi^{+-}_{\rm Born}(x,p)\Delta^{-+}_\pi(x,p)-\Pi^{-+}_{\rm Born}(x,p)\Delta^{+-}_\pi(x,p)]$$
$$=\int\frac{d^3p_2}{(2\pi)^3}\int\frac{d^3p_3}{(2\pi)^3}\int\frac{d^3p_4}{(2\pi)^3}(2\pi)^4\delta^{(4)}(p+p_2-p_3-p_4)W(p,p_2,p_3,p_4)(F_2-F_1); \tag{106}$$

here F_2,F_1 are again the Nordheim-Uehling-Uhlenbeck factors,

$$F_2=[1+f_\pi(\mathbf{x},\mathbf{p},\tau)][1\pm f_{H_2}(\mathbf{x},\mathbf{p}_2,\tau)]f_{H_3}(\mathbf{x},\mathbf{p}_3,\tau)f_{H_4}(\mathbf{x},\mathbf{p}_4,\tau), \tag{107}$$

$$F_1=f_\pi(\mathbf{x},\mathbf{p},\tau)f_{H_2}(\mathbf{x},\mathbf{p}_2,\tau)[1\pm f_{H_3}(\mathbf{x},\mathbf{p}_3,\tau)][1\pm f_{H_4}(\mathbf{x},\mathbf{p}_4,\tau)], \tag{108}$$

H_2,H_3,H_4 can be π, N, or Δ; the symbol $+$ assigns to bosons and $-$ to fermions. The transition probability $W(p,p_2,p_3,p_4)$ for different channels reads as

$$W_{\pi N\to\pi N}(p,p_2,p_3,p_4)=\frac{(g^\rho_{\pi\pi}g^\rho_{NN})^2}{16\omega^*(p)E^*(p_2)\omega^*(p_3)E^*(p_4)}T_a\Phi_a, \tag{109}$$

$$W_{\pi\Delta\to\pi\Delta}(p,p_2,p_3,p_4)=\frac{(g^\rho_{\pi\pi}g^\rho_{\Delta\Delta})^2}{16\omega^*(p)E^*_\Delta(p_2)\omega^*(p_3)E^*_\Delta(p_4)}T_b\Phi_b, \tag{110}$$

$$W_{\pi\pi\to\pi\pi}(p,p_2,p_3,p_4)=\frac{1}{16\omega^*(p)\omega^*(p_2)\omega^*(p_3)\omega^*(p_4)}\sum_{AB}[(g^A_{\pi\pi})^4T_c\Phi_c+(g^A_{\pi\pi}g^B_{\pi\pi})^2T_d\Phi_d]+p_3\leftrightarrow p_4, \tag{111}$$

where A, $B=\sigma,\rho$. Here T_{a-d} is the isospin matrix and Φ_{a-d} is the spin matrix. The subscripts a, b, c, d denote the terms contributed from Figs. 4(a)–4(d), respectively. The concrete expressions for T_{a-d} and Φ_{a-d} are

$$T_a=\sum_{t_2r_3t_4}\langle r|\tau^\pi_\rho|r_3\rangle\langle r_3|\tau^\pi_\rho|r\rangle\langle t_4|\tau_\rho|t_2\rangle\langle t_2|\tau_\rho|t_4\rangle D^i_\rho D^j_\rho, \tag{112}$$

$$T_b=\sum_{T_2r_3T_4}\langle r|\tau^\pi_\rho|r_3\rangle\langle r_3|\tau^\pi_\rho|r\rangle\langle T_4|T_\rho|T_2\rangle\langle T_2|T_\rho|T_4\rangle D^i_\rho D^j_\rho, \tag{113}$$

$$T_c=\sum_{r_2r_3r_4}\langle r|\tau^\pi_A|r_3\rangle\langle r_3|\tau^\pi_A|r\rangle\langle r_4|\tau^\pi_A|r_2\rangle\langle r_2|\tau^\pi_A|r_4\rangle D^i_A D^j_A, \tag{114}$$

$$T_d=\sum_{r_2r_3r_4}\langle r|\tau_A^\pi|r_4\rangle\langle r_4|\tau_B^\pi|r_2\rangle\langle r_2|\tau_A^\pi|r_3\rangle\langle r_3|\tau_B^\pi|r\rangle D_A^i D_B^j, \tag{115}$$

$$\Phi_a=(\gamma_\rho^\pi)^2 D_\rho^\mu D_\rho^\nu \mathrm{tr}[\gamma_\rho(\not p_2+m^*)\gamma_\rho(\not p_4+m^*)]\left[\frac{1}{(p-p_3)^2-m_\rho^2}\right]^2, \tag{116}$$

$$\Phi_b=(\gamma_\rho^\pi)^2 D_\rho^\mu D_\rho^\nu \mathrm{tr}[\gamma_\rho(\not p_2+m_\Delta^*)D^{\sigma\rho}(p_2)\gamma_\rho(\not p_4+m_\Delta^*)D_{\rho\sigma}(p_4)]\left[\frac{1}{(p-p_3)^2-m_\rho^2}\right]^2, \tag{117}$$

$$\Phi_c=(\gamma_A^\pi)^4 D_A^\mu D_A^\nu\left[\frac{1}{(p-p_3)^2-m_A^2}\right]^2, \tag{118}$$

$$\Phi_d=(\gamma_A^\pi\gamma_B^\pi)^2 D_A^\mu D_B^\nu\frac{1}{(p-p_3)^2-m_B^2}\frac{1}{(p-p_4)^2-m_A^2}. \tag{119}$$

We further express the right-hand side of Eq. (106) by the differential cross sections [77]

$$F_{\mathrm{el}}(x,p)=\int\frac{d^3p_2}{(2\pi)^3}v_\pi\sigma_\pi(s,t)(F_2-F_1)d\Omega; \tag{120}$$

here $\sigma_\pi(s,t)$ represents the in-medium differential cross sections of $\pi+N\to\pi+N,\pi+\Delta\to\pi+\Delta$, and $\pi+\pi\to\pi+\pi$ elastic scattering. Its concrete expressions can be obtained through computing Eqs. (112)–(119) and finally transforming it into the center-of-mass system. We give explicit expressions of $\sigma_{\pi N\to\pi N}(s,t),\sigma_{\pi\Delta\to\pi\Delta}(s,t)$, and $\sigma_{\pi\pi\to\pi\pi}(s,t)$ in Appendix C. After averaging over initial states, the in-medium total cross sections can be calculated through the following equations:

$$\sigma^*_{\pi N\to\pi N}=\frac{1}{4}\int\sigma_{\pi N\to\pi N}(s,t)d\Omega, \tag{121}$$

$$\sigma^*_{\pi\Delta\to\pi\Delta}=\frac{1}{16}\int\sigma_{\pi\Delta\to\pi\Delta}(s,t)d\Omega, \tag{122}$$

$$\sigma^*_{\pi\pi\to\pi\pi}=\frac{1}{6}\int\sigma_{\pi\pi\to\pi\pi}(s,t)d\Omega. \tag{123}$$

Of course, in calculating the $\sigma^*_{\pi\Delta\to\pi\Delta}$ one should also take the Δ-decay width into account. However, the strict treatment of Breit-Wigner distribution function as in Sec. IV might cause complexity in the derivation procedure since we are now concerning two Δ's in a scattering process. Practically, we usually introduce a centroid Δ mass in numerical calculations which can include the influence of Δ decay effectively. For a detailed description of the method we refer to Refs. [48,50,52]. At the end we can rewrite Eq. (62), the RVUU-type transport equation of the pion, in the following form:

$$\begin{aligned}&\left\{p^\mu\partial_\mu^x+\frac{1}{2}\partial_x^\mu\Pi_H(x)\partial_\mu^p+\frac{1}{2}\partial_x^\mu\mathrm{Re}\Pi^{--}_{\mathrm{loop}}(x,p)\partial_\mu^p\right.\\&\left.-\frac{1}{2}\partial_p^\mu\mathrm{Re}\Pi^{--}_{\mathrm{loop}}(x,p)\partial_\mu^x\right\}\frac{f_\pi(\mathbf{x},\mathbf{p},\tau)}{\omega^*(p)}\\&=\int\frac{d^3q}{(2\pi)^3}v\sigma_{\mathrm{abs}}(s)(F_2^0-F_1^0)\\&+\int\frac{d^3p_2}{(2\pi)^3}v_\pi\sigma_\pi(s,t)(F_2-F_1)d\Omega.\end{aligned} \tag{124}$$

The first term on the right-hand side of Eq. (124) stems from the $N\pi\to\Delta$ process (it is angle independent in the center-of-mass system) and the second term represents the π-hadron elastic scattering. It is of course interesting to investigate the π-hadron inelastic scattering processes, which may warrant further studies.

VI. NUMERICAL RESULTS AND DISCUSSIONS

In this section we present our numerical results for the in-medium pion dispersion relation, Δ-formation cross section, and momentum-dependent Δ-decay width. The calculations are performed in symmetric nuclear matter at zero temperature. The baryon distribution functions in Eqs. (75)–(78) and (93), (94) are replaced by the corresponding θ functions. The coupling strengths of $g^\sigma_{NN},g^\omega_{NN}$, and b, c, Z are determined by fitting the known ground-state properties for infinite nuclear matter. In this work we take parameter set 2 of Ref. [79], which gives $g^\sigma_{NN}=11.77$, $g^\omega_{NN}=13.88$, $b(g^\sigma_{NN})^3=13.447$, $c(g^\sigma_{NN})^4=10.395$, and $Z=3.655$. The corresponding saturation properties are the following: binding energy $E_{\mathrm{bin}}=-15.75$ MeV, saturated effective nucleon mass $m_N^*/M_N=0.6$, compressibility $K=200$ MeV, and saturation density $\rho_0=0.1484$ fm^{-3}.

For the coupling strengths of $g^\sigma_{\Delta\Delta}$ and $g^\omega_{\Delta\Delta}$, no direct information from experiments is available. For simplicity, we employ the argument of universal coupling strengths, i.e.,

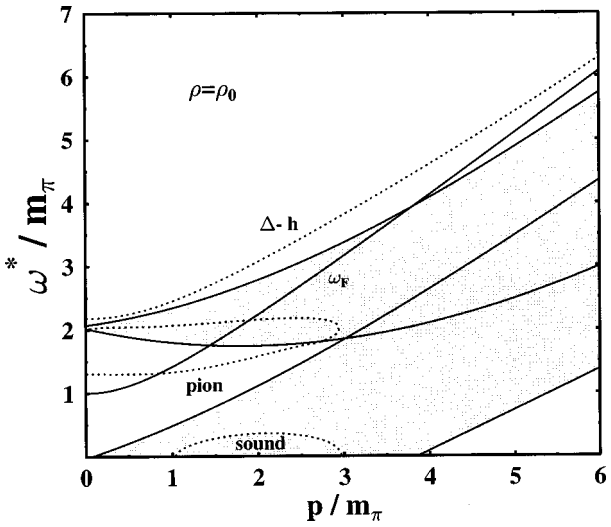

FIG. 6. The pion dispersion relation in symmetric nuclear matter at saturation density. The solid line shows the free dispersion relation. The dotted curves represent the in-medium dispersion relation for different branches as indicated in the figure. The upper and lower hatched areas indicate regions of nonvanishing imaginary parts of the Δ-hole and nucleon-hole polarizations, respectively.

$g^{\sigma}_{\Delta\Delta}=g^{\sigma}_{NN}$ and $g^{\omega}_{\Delta\Delta}=g^{\omega}_{NN}$ [80]. Other choices of the Δ coupling strengths now in the literature [61,81] are not considered here since they give unreasonable results for the pion dispersion relation. In this case, we do not have a nonzero Δ distribution in relativistic mean field calculations [79,81]. The contributions of Eqs. (76) and (78) to the real part of the pion self-energy vanish in the present calculations of the pion dispersion relation. It is, of course, not a realistic situation of the dynamical process of energetic heavy-ion collisions, where a rather large amount of nucleons are excited to the resonance states [67]. The contributions of Eqs. (76) and (78) will certainly enter the pion dispersion relation and might play an important role because of the large spin and isospin factors of the Δ resonance. Therefore, for the use of the in-medium pion dispersion relation presented in this work in the study of high-energy heavy-ion collisions, it should be viewed as a preliminary step approaching to the realistic description.

For the coupling strength of g^{π}_{NN}, we take the most commonly used value $f^2_{\pi}/4\pi=0.08$ [56]. The coupling strength of $g^{\pi}_{\Delta N}$ can be fixed through using Eq. (105) in free space. If one takes $M_N=939$ MeV, $M_{\Delta}=1232$ MeV, $m_{\pi}=138$ MeV, and the empirical value of $\Gamma_0=115$ MeV, it turns out $f^{*2}/4\pi=0.362$, very close to the commonly used value of 0.37 [40] [if one uses this value in Eq. (105), it gives $\Gamma_0=118$ MeV, still within the errorbar of experimental data]. In computing the real part of the pion self-energy we use a cutoff factor of $\Lambda^2=\exp(-2\mathbf{p}^2/b^2)$ with $b=7\ m_{\pi}$ as usually done [16,17].

A. In-medium pion dispersion relation

Figure 5 displays the gap between the effective masses of particles and antiparticles at different densities. One can see that the mass gap is much larger than the pion mass even at 3 times the normal density. That means that the antiparticles

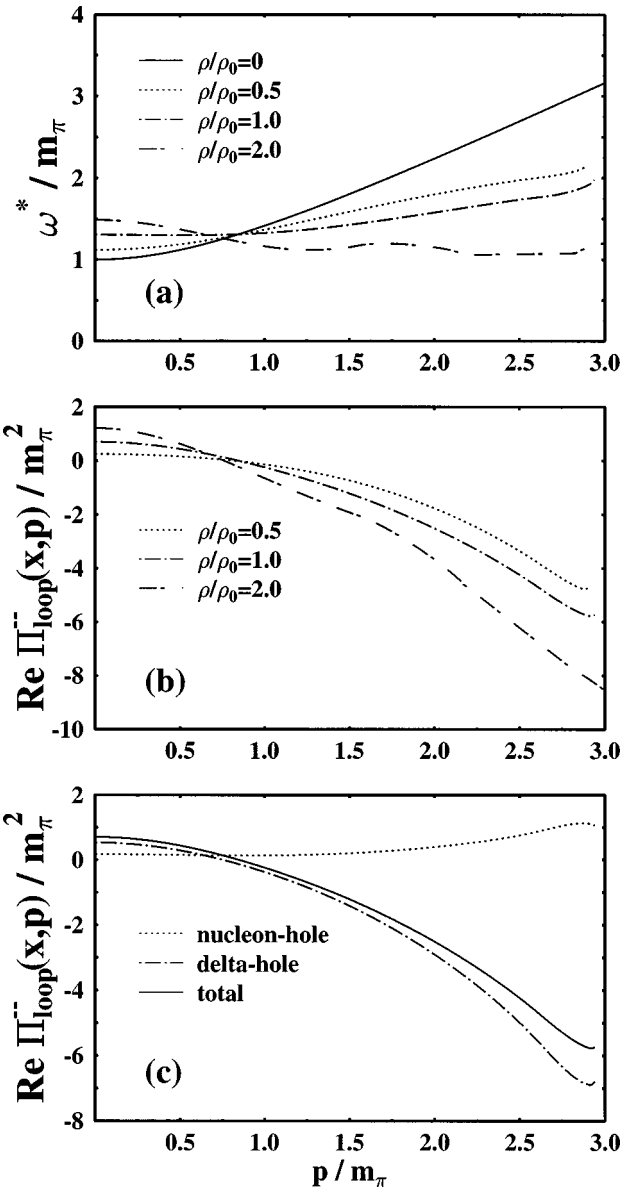

FIG. 7. (a) The pion dispersion relation at different densities. (b) The real part of pion self-energy at different densities relating to the pion dispersion relation shown in (a). (c) The contributions of different excitation modes to the real part of pion self-energy. The calculations are performed at normal density.

contribute only to the high branch of collective modes, which can be neglected in the present consideration.

Figure 6 depicts the in-medium pion dispersion relation calculated with Eq. (59) at normal density. Here we already drop the contribution of the Hartree term since we do not expect a large pion distribution at the energy and density considered. The areas of the nonvanishing imaginary part (NIP) of the pion self-energy are also indicated in the figure. The imaginary part of the pion self-energy in nuclear matter can be derived through inserting Eqs. (71) and (72) into Eqs. (65)–(68) and taking both the baryons on the mass shell. The analytical expressions are given in Appendix D. It should be pointed out that in calculating the pion dispersion relation of Eq. (59) self-consistency is realized only in the real part of the pion self-energy. From the figure one can find that the Δ-*h* branch is above the area of NIP. The sound branch is

buried in the region of the NIP contributed from the nucleon-hole excitation. For the pion branch, it first increases with the increase of momentum and then disappears in the region of the NIP contributed from the Δ-hole excitation when the momentum is larger than 3 times the pion mass. That means that at larger momenta the pion can be bounded in the Δ resonance. This scenario is commonly used in transport models. In the figure one can also find another dotted curve buried in the region of the NIP from Δ-hole excitation, which is related to the case that a formed Δ decays immediately.

Since we are mostly interested in the pion branch, in the following we discuss it in detail. In Fig. 7(a) we show the pion dispersion relation at different densities. The corresponding pion self-energy is displayed in Fig. 7(b). At $\rho = 2\rho_0$ one can see the numerical instability since at that density the pion self-energy is very large compared to the pion mass. Contrary to the results of the nonrelativistic model [16] where the pion branch always starts from the point of $\omega^* = m_\pi$ since the pion self-energy is an explicit function of $\mathbf{p}^2$ in that model, our results exhibit that the pion dispersion relation (pion branch) has a rather different behavior for different momenta. At lower momenta the pion has a positive self-energy, which causes the in-medium pion dispersion relation to be harder than the free one. The pion self-energy decreases with the increase of momentum. When p exceeds the point around 100 MeV the self-energy becomes negative and correspondingly the dispersion relation becomes softer than the free one. One may argue that nucleons are not very relativistic in nuclear matter; little difference is expected, for slow pions, between nonrelativistic and relativistic results. In Appendix E we reduce our relativistic formulas to the nonrelativistic limit. It is shown that the relativistic effect stemming from the Fermi motion of nucleons is negligible. But there does exist an evident difference to the nonrelativistic model mainly coming from the relativistic kinetics where p_μ^2 instead of $\mathbf{p}^2$ is used. The dispersion relation of Fig. 7(a) may provide a possible explanation of the pion spectrum over whole energy range. In Ref. [26] it was shown that the pion yield is overestimated at low momentum whereas it is underestimated at high momentum when a free dispersion relation was used. Figure 7(c) displays the contributions of different excitation modes to the real part of the pion self-energy. One can find the main contribution comes from the Δ-hole excitation as expected. The self-energy from the nucleon-hole excitation always has a positive value whereas the one from the Δ-hole excitation changes its sign from positive to negative at a certain momentum point, which controls the behavior of the pion dispersion relation.

The above calculations are performed through considering the lowest-order Feynman diagrams. Short-range correlations have not been included. In the nonrelativistic model, the short-range correlations are taken into account by means of the Migdal parameter g'. This method is frequently employed in the relativistic model [23] although it has never been checked carefully. We follow this way and take the pion self-energy under the random phase approximation as

$$\Pi'(p_\mu) = \frac{\mathrm{Re}\,\Pi^{--}_{\mathrm{loop}}(x,p)}{1+(g'/p_\mu^2)\,\mathrm{Re}\,\Pi^{--}_{\mathrm{loop}}(x,p)}. \tag{125}$$

With $g' = 0.6$ we have recalculated the pion dispersion relation which is plotted in Fig. 8. The behavior of the pion dispersion relation becomes quite strange and difficult to understand. Similar results were obtained in Ref. [23]. That might mean that it is unsuitable to incorporate short-range correlations in a relativistic model by means of a nonrelativistic approach. A fully self-consistent inclusion of correlation effects might be necessary, which is, however, quite complicated and needs to be discussed in a separate paper. Another possibility is that the effective Lagrangian of Eq. (19) might be valid only at lower order.

For a convenient use in the study of heavy-ion collisions, we parametrize the results of Fig. 7(a) as

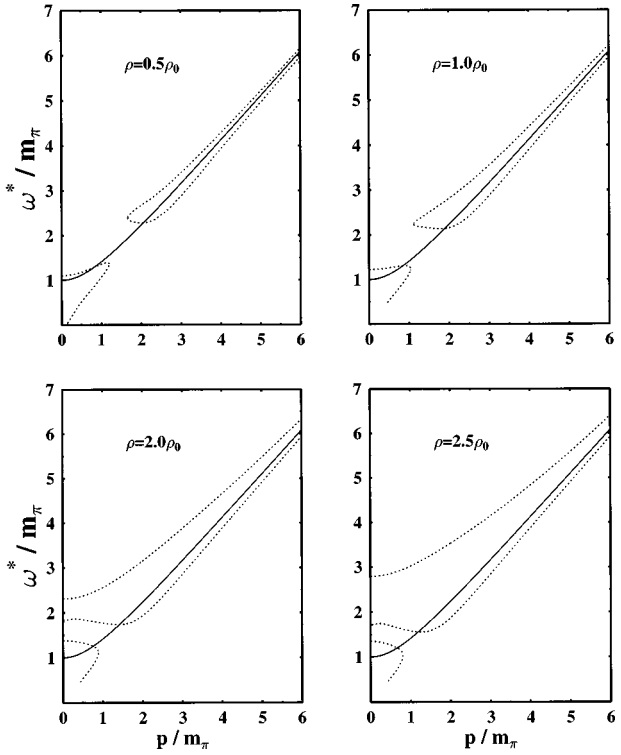

FIG. 8. The pion dispersion relation (dotted curves) at different densities. The short-range correlations are taken into account in a nonrelativistic way with Migdal parameter $g' = 0.6$. The solid lines represent the free dispersion relation.

$$\omega^* = \begin{cases} 1.10398 + 0.0790471p + 0.232015p^2 - 0.049101p^3, & \rho = 0.5\rho_0, \\ 1.32175 - 0.13706p + 0.165035p^2 - 0.0173563p^3, & \rho = \rho_0, \\ 1.56304 - 0.585238p + 0.261195p^2 - 0.0370091p^3, & \rho = 2\rho_0. \end{cases} \tag{126}$$

The unit of ω^* and p is m_π.

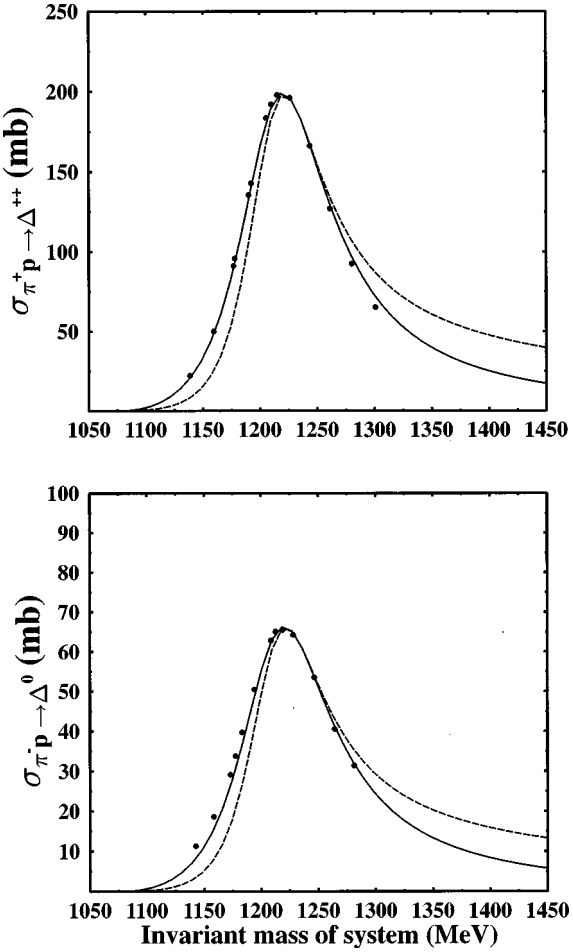

FIG. 9. Free cross sections for reactions $\pi^+ p \to \Delta^{++}$ and $\pi^- p \to \Delta^0$. The dots are the experimental data from Ref. [83]. The solid curve is our results calculated with the mass-dependent coupling strength while the dashed curve with the mass-independent coupling strength.

B. Δ-formation cross section and Δ-decay width

Now let us turn to the collision term of the pion transport equation. In this subsection we study the $\pi N \to \Delta$ cross section and the momentum-dependent Δ-decay width, which are the most important channels for pion absorption and production, both in free space and the nuclear medium. As has been pointed out in Sec. V, the Δ is a physically decaying particle. A Breit-Wigner function is commonly introduced to describe the broad width of the Δ resonance when one considers Δ-relevant scattering processes [19,48,76]. Consequently, the mass of the Δ has a distribution with respect to the total energy of the system. But in the framework of an effective field theory one only treats a point particle with fixed mass. If one introduces an energy-dependent mass, correspondingly, one should introduce certain corrections on the interaction vertex. Brueckner [82] suggested a vertex function of

$$F = \left(\frac{1 + R^2 (p_\pi^2)_0}{1 + R^2 p_\pi^2} \right)^{1/2} \tag{127}$$

to fit the phase shift of a broad resonance away from the resonance position. Here p_π is the relative momentum between nucleon and pion in the Δ-rest system. R is the radius of the boundary of the internal region. The typical value for the Δ is 0.98 fm [78]. In the same spirit a mixed version of the form factor for the $N\Delta\pi$ vertex was used in our previous works [48,50,52] which has essentially similar effects. More conveniently, here we phenomenologically introduce a mass-dependent coupling (MDC) strength $g^\pi_{\Delta N}(M_\Delta) = g^\pi_{\Delta N} F$, which will be used in the following calculations. The original coupling strength $g^\pi_{\Delta N}$ is afterwards referred to mass-independent coupling (MIC) strength.

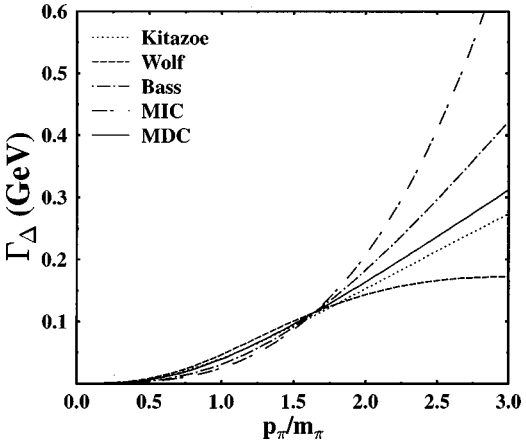

FIG. 10. The momentum-dependent Δ-decay width in free space. The solid line and long dash-dotted line are our results computed with MDC and MIC strengths, respectively. Dotted [84], dashed [85], and dash-dotted [86] lines represent several phenomenological parametrizations commonly used in the transport models.

Figure 9 displays the $\pi^+ p \to \Delta^{++}$ and $\pi^- p \to \Delta^0$ cross section in free space. The dots are the experimental data from Ref. [83]. The solid and dashed curves are our numerical results calculated with the mass-dependent (solid line) and mass-independent (dashed line) coupling strength, respectively. The results with MDC strength can reproduce the experimental data nearly perfectly. Furthermore, our calculations are almost parameter free. Only $g^\pi_{\Delta N}$ was fixed by fitting $\Gamma_0 = 115$ MeV. That implies that our theoretical framework for describing the pion is quite reasonable although it should be further checked in relativistic heavy-ion collisions.

In Fig. 10 we depict the momentum-dependent Δ-decay width in free space, calculated with MDC and MIC strengths, respectively. Some phenomenological parametrizations commonly used in the transport models are also presented in the figure. Our results with the MDC strength are comparable with these parametrizations. But the decay width calculated with the MIC strength increases very rapidly with the increase of the pion momentum, which will open the possibility that a Δ may have a mass much larger than its resonance mass [50]. This may not be the real case. In the following calculations we will use the mass-dependent coupling strength for the $N\Delta\pi$ vertex.

In Fig. 11 we show the in-medium Δ-formation cross section and Δ-decay width. The effective masses of nucleon and Δ are determined by Eqs. (87) and (88). The free pion mass is used in (a) and (b) while the effective pion mass from the dispersion relation of Fig. 7(a) is used in (c) and (d). From

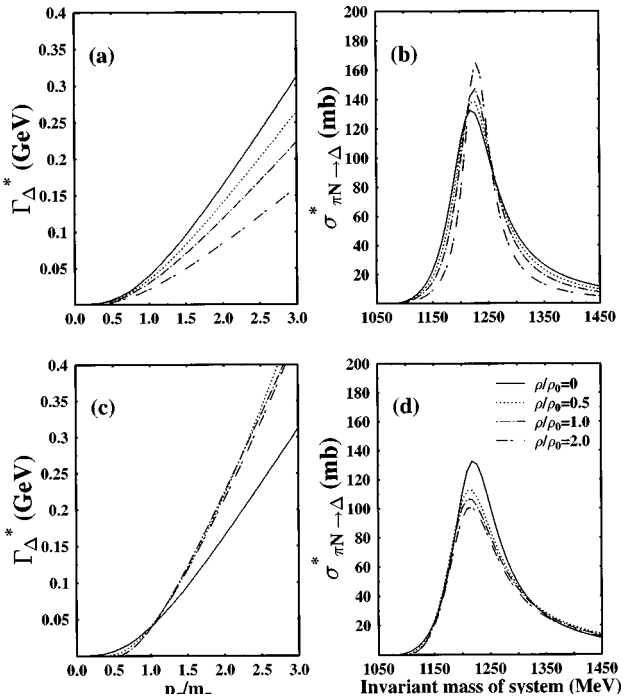

FIG. 11. The in-medium Δ-formation cross section and Δ-decay width. In (a) and (b) the free pion mass is used in the calculations. In (c) and (d) the effective pion mass is taken into account via the dispersion relation of Fig. 7(a).

the figure one can find the strong medium corrections. In the case of free pion mass, the effective Δ-decay width decreases rapidly with the increase of density. The Δ-formation cross section is enhanced near the Δ-resonance mass but suppressed at other region. The whole shape of curves becomes narrower compared to the free one. The in-medium Δ-decay width was studied by Kim *et al.* [87] where an effective pion mass stemming from the nucleon-hole excitation was used. This kind of effective mass is very close to the free mass as stated in their paper, and might be seen from Fig. 7(c). They obtained a suppressed Δ-decay width at normal density which is in qualitative agreement with our results. However, in our calculations the Pauli blocking of the final nucleon is not taken into account; so a quantitative comparison is not possible. The Pauli blocking is of course incorporated in the transport equation (124). The effects of Pauli blocking alone on the in-medium resonance decay width were investigated by Effenberger *et al.* in Ref. [88].

In Figs. 11(c) and 11(d) the medium effects on the pion are incorporated. Compared to Figs. 11(a) and 11(b) one can find that the effective mass of the pion can change the results completely, even the trend of the density dependence. It seems that if the smaller effective mass of the pion is taken into account, the in-medium Δ-decay width increases as compared to the free mass. The medium effects on the Δ-formation cross section are now exhibited to be important only in the region where the formed Δ has the mass around the Δ-resonance mass. It decreases with the increase of density. When the formed Δ is far away from its resonance mass, the medium corrections to the Δ-formation cross section are negligible.

VII. SUMMARY AND OUTLOOK

A large amount of data with high accuracy for the pion spectrum and pion flow has been accumulated. A π-beam facility will be available at GSI which will provide new and specific data to help to understand the pion dynamics in relativistic heavy-ion collisions. However, a self-consistent treatment of pions, together with the nucleons and Δ's, is still not realized in current transport models. In view of this fact, we have developed a RVUU-type transport equation for the pion distribution function based on an effective Lagrangian of the QHD-II model [56]. The closed-time-path Green's function technique is employed and the semiclassical, quasiparticle, and Born approximations are adopted in our derivation. We have presented an unified approach to the following problems: First, both the mean field (the real part of the pion self-energy) and the collision term (the imaginary part of the pion self-energy) of the transport equation are derived simultaneously from the same effective Lagrangian and presented analytically. Second, we treat the real pion and virtual pion on the same footing. Third, the transport equation of pion is derived within the same framework which we applied to the nucleon [15,47–49,52] and Δ [50,51] before. Therefore, we obtain a set of coupled equations for the N, Δ, and π system which describes the hadronic matter in an unified way.

Within this approach we have investigated the in-medium pion dispersion relation. In contrast to the results of the nonrelativistic model where a softer dispersion relation over the whole momentum range is exhibited, the predicted in-medium dispersion relation turns out to be harder at lower momenta and softer at higher momenta, compared to the free one. The main reason for the difference relies on the fact that in our relativistic model the pion self-energy has a relativistic kinetics p_μ while in the nonrelativistic model it explicitly depends on three-momentum $\mathbf{p}$ [40], in which the real part of the pion self-energy goes to zero when $\mathbf{p}\to 0$. However, a pion in the nuclear medium should in principle suffer the interaction of surrounding particles, whatever it moves or not. In our calculations the real part of the pion self-energy has a positive value at smaller momenta [89]. Consequently, the momentum dependence of the in-medium pion dispersion relation becomes very flat and quite different from the free one and that of the nonrelativistic model. This will certainly have effects on the pion spectrum and pion flow as well as on the dilepton production since one of the important channels $\pi^+\pi^-\to\rho\to e^+e^-$ explicitly depend on the slope of $d\omega/dp$ [27]. It would be very interesting to check this kind of pion dispersion relation in the dynamical processes of relativistic heavy-ion collisions. Work on this aspect is in progress.

Considering that in the nuclear medium the absorption and production of pions are mostly realized through the formation and decay of the Δ resonance, we have studied the Δ-formation cross section and Δ-decay width both in free space and in the medium. Our theoretical prediction for the free Δ-formation cross section is nearly in perfect agreement with the experimental data. The computed free Δ-decay width is comparable to several phenomenological parametrizations commonly used in transport models. It is found that the effective pion mass has a strong influence on the predicted in-medium Δ-formation cross section and Δ-decay

width. It can even change the trend of the density dependence. After taking into account the medium corrections on the nucleon, Δ, and pion mass simultaneously, the Δ-decay width turns out to be enhanced in the medium especially at higher momenta, while the Δ-formation cross section is suppressed around the resonance mass. When the formed Δ is far away from its resonance mass, the medium effects on the Δ-formation cross section are negligible.

In investigating the in-medium pion dispersion relation we have taken into account only the lowest-order diagrams stemming from the nucleon-hole and Δ-hole excitation. The effects of short-range correlations have been addressed through following the method of the nonrelativistic model with Migdal parameter g'. But the results turn out to be quite strange. In fact, short-range correlations can be considered in a relativistic model self-consistently by implementing correlation terms like $(\bar{\psi}\gamma_\mu\gamma_5\boldsymbol{\tau}\psi)^2$ and $(\bar{\psi}_{\Delta\mu}\mathbf{S}^+\psi)^2$ in the effective Lagrangian of Eq. (19). In the mean field approximation one should calculate the expectation value of $\langle\bar{\psi}\gamma_\mu\gamma_5\boldsymbol{\tau}\psi\rangle$ and $\langle\bar{\psi}_{\Delta\mu}\mathbf{S}^+\psi\rangle$ which corresponds to the condensate of the pion field. Although a detailed investigation of correlation effects may go beyond the scope of the RVUU approach, it is nevertheless very interesting to check the effects of short-range correlations on the pion dispersion relation even in static nuclear matter within a relativistic model self-consistently. It would be extremely interesting if this collective instability could be studied in a dynamical situation.

As usually done in a microscopic transport theory for nonequilibrium system, the temperature degree of freedom is not taken into account in the present work. One might consider the temperature degree of freedom in nuclear matter by simply replacing the single-particle distribution functions with the Fermi-Dirac (for fermions) and Bose-Einstein (for bosons) distribution functions. In this way one can study the effects of temperature on the predicted quantities. This is especially meaningful in the present case since the Δ distribution will enter explicitly at certain temperatures [79]. Then the $\Delta\Delta^{-1}$ and $N\Delta^{-1}$ excitations of Figs. 3(c), 3(d) and 3(g), 3(h) might play an important role on the in-medium pion dispersion relation. This would be more close to the realistic situation of energetic heavy-ion collisions and requires further studies.

As frequently emphasized in this paper, up to now we only treat the pion as a real particle. Other mesons such as σ,ω, and ρ still remain virtual ones. It is of course interesting to develop transport equations for ω and ρ mesons as well as for other experimental observable mesons K, $K^*,\eta,\phi,\ldots$ within the present framework. Among them, the ρ meson is especially important for dilepton production which cannot be explained by current transport models. Medium corrections to the properties of ω and ρ as well as η mesons may provide a possible explanation [32–34,90–92].

In almost all practically used RVUU-type transport calculations, the local-density approximation is employed in order to realize the numerical solution of the equation. This drops the retardation effects of the mean field, although the equation itself is constructed from the relativistic model. From Eq. (2) one can find that it is possible to describe the propagation of real as well as virtual σ and ω mesons simultaneously. In this case one can obtain the time-dependent mean field and the transport equations for the σ and ω distribution functions at the same time. It would be interesting to study this problem and explore it just from a theoretical point of view.

ACKNOWLEDGMENTS

The authors thank C. Ernst and I.N. Mishustin for fruitful discussions. G.M. is grateful to the Alexander von Humboldt-Stiftung for financial support and to the people at the Institut für Theoretische Physik der J. W. Goethe Universität for their hospitality. This work was supported by DFG-Graduiertenkolleg Theoretische & Experimentelle Schwerionenphysik, GSI, BMBF, DFG and A.v.Humboldt-Stiftung.

APPENDIX A

In this appendix we present the zeroth-order Green's functions of nucleon, Δ, and mesons used in this work.

(1) Nucleon:

$$\langle T[\psi(1)\bar{\psi}(2)]\rangle = iG^0(1,2)\,\delta_{t_1,t_2'}, \tag{A1}$$

$$iG^0(1,2) = i\int\frac{d^4k}{(2\pi)^4}G^0(x,k)e^{-ik(x_1-x_2)}, \tag{A2}$$

$$G^{0\mp\mp}(x,k) = (\not{k}+M_N)\left[\frac{\pm 1}{k^2-M_N^2\pm i\epsilon} + \frac{\pi i}{E(k)}\delta[k_0-E(k)]f(x,k)\right], \tag{A3}$$

$$G^{0+-}(x,k) = -\frac{\pi i}{E(k)}\delta[k_0-E(k)][1-f(x,k)](\not{k}+M_N), \tag{A4}$$

$$G^{0-+}(x,k) = \frac{\pi i}{E(k)}\delta[k_0-E(k)]f(x,k)(\not{k}+M_N). \tag{A5}$$

(2) Delta:

$$\langle T[\psi_{\Delta\mu}(1)\bar{\psi}_{\Delta\nu}(2)]\rangle = -iG^0_{\mu\nu}(1,2)\,\delta_{T_1,T_2'}, \tag{A6}$$

$$iG^0_{\mu\nu}(1,2) = i\int\frac{d^4k}{(2\pi)^4}G^0_{\mu\nu}(x,k)e^{-ik(x_1-x_2)}, \tag{A7}$$

$$G^{0\mp\mp}_{\mu\nu}(x,k) = (\not{k}+M_\Delta)D_{\mu\nu}\left[\frac{\pm 1}{k^2-M_\Delta^2\pm i\epsilon} + \frac{\pi i}{E(k)}\delta[k_0-E(k)]f_\Delta(x,k)\right], \tag{A8}$$

$$G^{0+-}_{\mu\nu}(x,k) = -\frac{\pi i}{E(k)}\delta[k_0-E(k)] \times[1-f_\Delta(x,k)](\not{k}+M_\Delta)D_{\mu\nu}, \tag{A9}$$

$$G^{0-+}_{\mu\nu}(x,k)=\frac{\pi i}{E(k)}\delta[k_0-E(k)]f_\Delta(x,k)(\not k+M_\Delta)D_{\mu\nu}, \tag{A10}$$

$$D_{\mu\nu}=g_{\mu\nu}-\frac{1}{3}\gamma_\mu\gamma_\nu-\frac{1}{3M_\Delta}(\gamma_\mu k_\nu-\gamma_\nu k_\mu)-\frac{2}{3M_\Delta^2}k_\mu k_\nu. \tag{A11}$$

(3) Mesons:

$$\langle T[\Phi_A(1)\Phi_B(2)]\rangle=iD_A\Delta^0_A(1,2)\delta_{AB}, \tag{A12}$$

where $A, B=\sigma,\omega,\pi,\rho$,

$$D_A=D^\mu_A D^i_A, \tag{A13}$$

D^μ_A and D^i_A are defined and listed in Table I, and

$$i\Delta^0_A(1,2)=i\int\frac{d^4k}{(2\pi)^4}\Delta^0_A(x,k)e^{-ik(x_1-x_2)}, \tag{A14}$$

$$\Delta^{0\mp\mp}_A(x,k)=\frac{\pm1}{k^2-m_A^2\pm i\epsilon}-2\pi i\delta[k^2-m_A^2]f_A(x,k), \tag{A15}$$

$$\Delta^{0\pm\mp}_A(x,k)=-2\pi i\delta[k^2-m_A^2][\theta(\pm k_0)+f_A(x,k)]. \tag{A16}$$

Here the numbers 1, 2 represent x_1,x_2. t_1,t_2' denote the isospin of nucleons and T_1,T_2' denote those of Δ's. $f(x,k)$, $f_\Delta(x,k)$, and $f_A(x,k)$ are nucleon, Δ and meson distribution functions, respectively. The abbreviation for isospin on the distribution function has been suppressed.

APPENDIX B

In this appendix we perform the Wigner transformation of Eq. (45), which can be easily realized by means of the following formulas [73]:

$$\partial^\mu_x f(x,y)\rightarrow\left(-iP^\mu+\frac{1}{2}\partial^\mu\right)f(X,P), \tag{B1}$$

$$\partial^\mu_y f(x,y)\rightarrow\left(iP^\mu+\frac{1}{2}\partial^\mu\right)f(X,P), \tag{B2}$$

$$h(x)g(x,y)\rightarrow h(X)g(X,P)-\frac{i}{2}\frac{\partial h(X)}{\partial X^\mu}\frac{\partial g(X,P)}{\partial P_\mu}, \tag{B3}$$

$$h(y)g(x,y)\rightarrow h(X)g(X,P)+\frac{i}{2}\frac{\partial h(X)}{\partial X^\mu}\frac{\partial g(X,P)}{\partial P_\mu}, \tag{B4}$$

$$\int d^4x' f(x,x')g(x',y)\rightarrow f(X,P)g(X,P)+\frac{i}{2}\left[\frac{\partial f(X,P)}{\partial P_\mu}\frac{\partial g(X,P)}{\partial X^\mu}-\frac{\partial f(X,P)}{\partial X^\mu}\frac{\partial g(X,P)}{\partial P_\mu}\right]; \tag{B5}$$

here

$$X=\frac{1}{2}(x+y). \tag{B6}$$

After Wigner transformation the different terms in Eq. (45) turn out to be

$$\partial^1_\mu\partial^\mu_1\Delta^{-+}_\pi(1,2)\rightarrow\left(\frac{1}{4}\partial^X_\mu\partial^\mu_X-iP^\mu\partial^X_\mu-P^2\right)\Delta^{-+}_\pi(X,P), \tag{B7}$$

$$\Pi_H(1)\Delta^{-+}_\pi(1,2)\rightarrow\Pi_H(X)\Delta^{-+}_\pi(X,P)-\frac{i}{2}\partial^\mu_X\Pi_H(X)\partial^P_\mu\Delta^{-+}_\pi(X,P), \tag{B8}$$

$$\mathrm{Re}\,\Pi^{--}_{\mathrm{loop}}(1,3)\Delta^{-+}_\pi(3,2)\rightarrow\mathrm{Re}\,\Pi^{--}_{\mathrm{loop}}(X,P)\Delta^{-+}_\pi(X,P)+\frac{i}{2}[\partial^\mu_P\,\mathrm{Re}\,\Pi^{--}_{\mathrm{loop}}(X,P)\partial^X_\mu\Delta^{-+}_\pi(X,P)-\partial^\mu_X\,\mathrm{Re}\,\Pi^{--}_{\mathrm{loop}}(X,P)\partial^P_\mu\Delta^{-+}_\pi(X,P)], \tag{B9}$$

$$\Pi^{+-}_{\mathrm{coll}}(1,3)\Delta^{-+}_\pi(3,2)\rightarrow\Pi^{+-}_{\mathrm{coll}}(X,P)\Delta^{-+}_\pi(X,P). \tag{B10}$$

In Eq. (B10) we have dropped the contributions from derivative terms. That means that collisions are performed at instantaneous time: *Boltzmann ansatz* [54,72].

APPENDIX C

In this appendix we present analytical expressions of in-medium differential cross sections for π-hadron elastic scattering. (a) Differential cross section of in-medium $\pi N\rightarrow\pi N$ scattering:

$$\sigma_{\pi N\to\pi N}(s,t)=\frac{1}{(2\pi)^2 s}\frac{(g_{\rho\pi}g^{\rho}_{NN})^2}{2(t-m_\rho^2)^2}[(m^{*2}+m_\pi^{*2}-2s)(m^{*2}+m_\pi^{*2})+s^2+st-m^{*2}t], \tag{C1}$$

where

$$s=(p+p_2)^2=[\omega^*(p)+E^*(p_2)]^2-(\mathbf{p}+\mathbf{p}_2)^2, \tag{C2}$$

$$t=\frac{1}{2}(2m^{*2}+2m_\pi^{*2}-s)-\frac{1}{2s}(m^{*2}-m_\pi^{*2})^2+2|\mathbf{p}||\mathbf{p}_3|\cos\theta, \tag{C3}$$

$$|\mathbf{p}|=|\mathbf{p}_3|=\frac{1}{2\sqrt{s}}\sqrt{(s-m^{*2}-m_\pi^{*2})^2-4m_\pi^{*2}m^{*2}}, \tag{C4}$$

and θ is the scattering angle in c.m. system.

(b) Differential cross section of in-medium $\pi\Delta\to\pi\Delta$ scattering:

$$\sigma_{\pi\Delta\to\pi\Delta}(s,t)=\frac{1}{(2\pi)^2 s}\frac{5(g_{\rho\pi}g^{\rho}_{\Delta\Delta})^2}{36m_\Delta^{*4}(t-m_\rho^2)^2}[18m_\Delta^{*4}(m_\Delta^{*2}+m_\pi^{*2})^2-2m_\Delta^{*6}(18s+11t)-m_\Delta^{*4}(36m_\pi^{*2}s+16m_\pi^{*2}t-18s^2-26st-7t^2)+m_\Delta^{*2}(8m_\pi^{*2}st-4m_\pi^{*4}t+2m_\pi^{*2}t^2-4s^2t-6st^2-t^3)+m_\pi^{*2}t^2(m_\pi^{*2}-2s)+st^2(s+t)], \tag{C5}$$

where

$$s=(p+p_2)^2=[\omega^*(p)+E_\Delta^*(p_2)]^2-(\mathbf{p}+\mathbf{p}_2)^2, \tag{C6}$$

$$t=\frac{1}{2}(2m_\Delta^{*2}+2m_\pi^{*2}-s)-\frac{1}{2s}(m_\Delta^{*2}-m_\pi^{*2})^2+2|\mathbf{p}||\mathbf{p}_3|\cos\theta, \tag{C7}$$

$$|\mathbf{p}|=|\mathbf{p}_3|=\frac{1}{2\sqrt{s}}\sqrt{(s-m_\Delta^{*2}-m_\pi^{*2})^2-4m_\pi^{*2}m_\Delta^{*2}}. \tag{C8}$$

(c) Differential cross section of in-medium $\pi\pi\to\pi\pi$ scattering:

$$\sigma_{\pi\pi\to\pi\pi}(s,t)=\frac{1}{(2\pi)^2 s}[D(s,t)+E(s,t)+(s,t\leftrightarrow u)], \tag{C9}$$

$$D(s,t)=\frac{3(g_{\sigma\pi}m_\sigma)^4}{256(t-m_\sigma^2)^2}+\frac{(g_{\rho\pi})^4}{4(t-m_\rho^2)^2}(4m_\pi^{*2}-2s-t)^2, \tag{C10}$$

$$E(s,t)=\frac{(g_{\sigma\pi}m_\sigma)^4}{256(t-m_\sigma^2)(u-m_\sigma^2)}+\frac{(g_{\rho\pi})^4}{8(t-m_\rho^2)(u-m_\rho^2)}(s-t)(2s+t-4m_\pi^{*2})+\left(\frac{1}{2}g_{\sigma\pi}m_\sigma g_{\rho\pi}\right)^2\left[\frac{4m_\pi^{*2}-2s-t}{8(t-m_\rho^2)(u-m_\sigma^2)}+\frac{t-s}{8(t-m_\sigma^2)(u-m_\rho^2)}\right], \tag{C11}$$

where the function D represents the contribution of the direct term, E is the exchange term, and

$$s=(p+p_2)^2=[\omega^*(p)+\omega^*(p_2)]^2-(\mathbf{p}+\mathbf{p}_2)^2, \tag{C12}$$

$$t=\frac{1}{2}(4m_\pi^{*2}-s)+2|\mathbf{p}||\mathbf{p}_3|\cos\theta, \tag{C13}$$

$$u=4m_\pi^{*2}-s-t, \tag{C14}$$

$$|\mathbf{p}|=|\mathbf{p}_3|=\frac{1}{2}\sqrt{s-4m_\pi^{*2}}. \tag{C15}$$

APPENDIX D

In this appendix we present analytical expressions of the imaginary part of the pion self-energy in nuclear matter.

(a) For spacelike p_μ,

$$\mathrm{Im}\,\Pi^{--}_{NN^{-1}}(x,p)=\frac{m^{*2}p_\mu^2}{\pi|\mathbf{p}|}(g^{\pi}_{NN})^2(E_F-E^*), \tag{D1}$$

where

$$E_F=(m^{*2}+k_F^2)^{1/2}, \tag{D2}$$

$$E^*=\min(E_F,E_{\max}), \tag{D3}$$

$$E_{\max}=\max\left[m^*,E_F-|p_0|,-\frac{1}{2}|p_0|+\frac{1}{2}|\mathbf{p}|\left(1-\frac{4m^{*2}}{p_\mu^2}\right)^{1/2}\right], \tag{D4}$$

$$\mathrm{Im}\,\Pi^{--}_{\Delta\Delta^{-1}}(x,p)=\frac{5p_\mu^2}{18\pi|\mathbf{p}|m_\Delta^{*2}}(p_\mu^4-2p_\mu^2m_\Delta^{*2}+10m_\Delta^{*4})(g^\pi_{\Delta\Delta})^2(E_F^\Delta-E_\Delta^*), \quad \text{(D5)}$$

and

$$E_F^\Delta=[m_\Delta^{*2}+(k_F^\Delta)^2]^{1/2}, \quad \text{(D6)}$$

$$E_\Delta^*=\min(E_F^\Delta,E_{\max}^\Delta), \quad \text{(D7)}$$

$$E_{\max}^\Delta=\max\left[m_\Delta^*,E_F^\Delta-|p_0|,-\frac{1}{2}|p_0|+\frac{1}{2}|\mathbf{p}|\times\left(1-\frac{4m_\Delta^{*2}}{p_\mu^2}\right)^{1/2}\right], \quad \text{(D8)}$$

$$\mathrm{Im}\,\Pi^{--}_{\Delta N^{-1}}(x,p)=\frac{(g^\pi_{\Delta N})^2}{12\pi|\mathbf{p}|}C(p,q)(E_F-E^*), \quad \text{(D9)}$$

where

$$E^*=\min(E_F,E_{\max}), \quad \text{(D10)}$$

$$E_{\max}=\max\left[m^*,E_F^\Delta-|p_0|,-\frac{1}{2}|p_0|\epsilon+\frac{1}{2}|\mathbf{p}|\left(\epsilon^2-\frac{4m^{*2}}{p_\mu^2}\right)^{1/2}\right], \quad \text{(D11)}$$

and

$$\epsilon=\frac{p_\mu^2+m^{*2}-m_\Delta^{*2}}{p_\mu^2}, \quad \text{(D12)}$$

$$C(p,q)=\frac{1}{3m_\Delta^{*2}}[p_\mu^2-(m_\Delta^*-m^*)^2][p_\mu^2-(m_\Delta^*+m^*)^2]^2. \quad \text{(D13)}$$

The definition of E_F and E_F^Δ is the same as in Eqs. (D2) and (D6):

$$\mathrm{Im}\,\Pi^{--}_{N\Delta^{-1}}(x,p)=\frac{(g^\pi_{\Delta N})^2}{12\pi|\mathbf{p}|}C(p,q)(E_F^\Delta-E^*), \quad \text{(D14)}$$

where

$$E^*=\min(E_F^\Delta,E_{\max}), \quad \text{(D15)}$$

$$E_{\max}=\max\left[m_\Delta^*,E_F-|p_0|,-\frac{1}{2}|p_0|\epsilon'+\frac{1}{2}|\mathbf{p}|\left(\epsilon'^2-\frac{4m_\Delta^{*2}}{p_\mu^2}\right)^{1/2}\right], \quad \text{(D16)}$$

and

$$\epsilon'=\frac{p_\mu^2+m_\Delta^{*2}-m^{*2}}{p_\mu^2}. \quad \text{(D17)}$$

(b) For timelike p_μ,

$$\mathrm{Im}\,\Pi^{--}_{\Delta N^{-1}}(x,p)=\begin{cases}\dfrac{(g^\pi_{\Delta N})^2}{12\pi|\mathbf{p}|}C(p,q)(E_u-E_d), & 0\leqslant p_\mu^2\leqslant(m_\Delta^*-m^*)^2,\\ 0, & \text{otherwise,}\end{cases} \quad \text{(D18)}$$

where

$$E_u=\min\left[E_F,-\frac{1}{2}|p_0|\epsilon+\frac{1}{2}|\mathbf{p}|\left(\epsilon^2-\frac{4m^{*2}}{p_\mu^2}\right)^{1/2}\right], \quad \text{(D19)}$$

$$E_d=\min(E_F,E_{\max}), \quad \text{(D20)}$$

$$E_{\max}=\max\left[m^*,E_F^\Delta-|p_0|,-\frac{1}{2}|p_0|\epsilon-\frac{1}{2}|\mathbf{p}|\left(\epsilon^2-\frac{4m^{*2}}{p_\mu^2}\right)^{1/2}\right]. \quad \text{(D21)}$$

For the timelike p_μ, the contributions of $\mathrm{Im}\,\Pi^{--}_{NN^{-1}}(x,p)$ and $\mathrm{Im}\,\Pi^{--}_{\Delta\Delta^{-1}}$, which describe the particle-antiparticle decay processes, vanish since we neglect the antiparticles in the present framework. In this work the numerical calculations are performed in cold nuclear matter with the assumption of chemical equilibrium, i.e., $E_F^\Delta=E_F$ when a Δ is produced. In this case the Δ-decay process is Pauli blocked since a Δ can only decay into a pion and a nucleon with a momentum smaller than the nucleon Fermi momentum, which leads to $\mathrm{Im}\,\Pi^{--}_{N\Delta^{-1}}(x,p)=0$ when $p_0>|\mathbf{p}|$.

APPENDIX E

In this appendix we introduce the nonrelativistic approximation for Eqs. (75) and (77). These two terms stemming from the particle-hole and Δ-hole excitations are commonly considered in the nonrelativistic approach [40,16,21]. The effective masses and energies in the expressions are replaced by the corresponding free ones. In order to make a complete nonrelativistic

reduction we have to start from the full Green's functions including the contribution of antiparticles. Equations (75) and (77) then read as

$$\mathrm{Re}\,\Pi^{--}_{NN^{-1}}(x,p)=2(g^{\pi}_{NN})^2\int\frac{d^3q}{(2\pi)^3}\left[\frac{A(p,q)}{2E(q)}\frac{f(\mathbf{x},\mathbf{q},\tau)}{[p_0+E(q)]^2-E^2(p+q)}+p_\mu\rightarrow-p_\mu\right], \tag{E1}$$

$$\mathrm{Re}\,\Pi^{--}_{\Delta N^{-1}}(x,p)=-\frac{4}{3}(g^{\pi}_{\Delta N})^2\int\frac{d^3q}{(2\pi)^3}\left[\frac{C(p,q)}{2E(q)}\frac{f(\mathbf{x},\mathbf{q},\tau)}{[p_0+E(q)]^2-E^2_\Delta(p+q)}+p_\mu\rightarrow-p_\mu\right], \tag{E2}$$

with the $A(p,q)$ and $C(p,q)$ defined by Eqs. (79) and (83). After some algebra we obtain

$$\mathrm{Re}\,\Pi^{--}_{NN^{-1}}(x,p)=-4(g^{\pi}_{NN})^2\int\frac{d^3q}{(2\pi)^3}\frac{M_N^2p_\mu^2}{E^2(q)}\left[\frac{f(\mathbf{x},\mathbf{q},\tau)}{p_\mu^2/2E(q)-\mathbf{p}\cdot\mathbf{q}/E(q)+p_0}+p_\mu\rightarrow-p_\mu\right], \tag{E3}$$

$$\begin{aligned}\mathrm{Re}\,\Pi^{--}_{\Delta N^{-1}}(x,p)=\frac{8}{9}(g^{\pi}_{\Delta N})^2\int\frac{d^3q}{(2\pi)^3}\frac{f(\mathbf{x},\mathbf{q},\tau)}{E(q)}\Bigg[&\frac{(p\cdot q)^2-M_N^2p_\mu^2}{M_\Delta^2}+\frac{2p_\mu^2M_N(M_\Delta+M_N)}{M_\Delta^2}\\&+\frac{(p\cdot q)^2-M_N^2p_\mu^2}{2M_\Delta^2E(q)}\frac{(M_\Delta+M_N)^2-p_\mu^2}{p_\mu^2/2E(q)-\mathbf{p}\cdot\mathbf{q}/E(q)-(M_\Delta^2-M_N^2)/2E(q)+p_0}+p_\mu\rightarrow-p_\mu\Bigg],\end{aligned} \tag{E4}$$

which are the same as Eqs. (8) and (11) in Ref. [14]. Taking the nonrelativistic limit $E(q)\approx M_N$, Eq. (E3) becomes

$$\mathrm{Re}\,\Pi^{--}_{NN^{-1}}(x,p)=(g^{\pi}_{NN})^2p_\mu^2\frac{2\omega_p}{p_0^2-\omega_p^2}\rho_N, \tag{E5}$$

with $\omega_p=p_\mu^2/2M_N$. If one further neglects the relativistic kinematics, i.e., $p_\mu^2\rightarrow-\mathbf{p}^2$, it returns to the standard nonrelativistic formula stemming from the particle-hole excitation [40,16]. Therefore, the relativistic effects stay in two aspects: one is the Fermi motion of nucleons in a nucleus which is small; that other one is the relativistic kinetics which turns out to be substantial in our calculations as can be seen later. In the nonrelativistic limit, Eq. (E4) becomes

$$\begin{aligned}\mathrm{Re}\,\Pi^{--}_{\Delta N^{-1}}(x,p)=&\frac{4}{9}(g^{\pi}_{\Delta N})^2\frac{M_N\mathbf{p}^2}{M_\Delta^2}\rho_N\\&+\frac{8}{9}(g^{\pi}_{\Delta N})^2\frac{(M_\Delta+M_N)}{M_\Delta^2}p_\mu^2\rho_N\\&-\frac{1}{9}(g^{\pi}_{\Delta N})^2\frac{(M_\Delta+M_N)^2-p_\mu^2}{M_\Delta^2}\frac{2\omega_R}{p_0^2-\omega_R^2}\mathbf{p}^2\rho_N,\end{aligned} \tag{E6}$$

with

$$\omega_R=\frac{p_\mu^2}{2M_N}-\frac{M_\Delta^2-M_N^2}{2M_N}. \tag{E7}$$

The first and second terms on the right-hand side (RHS) of Eq. (E6) are the nonresonant terms, which have no analogy in the nonrelativistic model. The third term can be reduced ($p_\mu^2\rightarrow-\mathbf{p}^2$) to a similar term in the nonrelativistic model stemming from the Δ-hole excitation, but there exist some differences mainly caused by the different masses of nucleons and Δ's. The situation might be understood in view of the fact that the problem of describing a spin-3/2 particle in relativistic quantum field theory remains unsolved. Fortunately, the difference between the nonrelativistic limit of the relativistic model and the standard nonrelativistic model is quantitatively insubstantial.

Figure 12(a) displays the pion dispersion relation (the pion branch) at normal density. The solid line denotes the free pion dispersion relation. The dotted line is calculated with Eqs. (E5) and (E6), i.e., the nonrelativistic limit of the relativistic model, but with the relativistic kinetics. The dashed line is computed by taking $p_\mu^2\rightarrow-\mathbf{p}^2$ in Eqs. (E5) and (E6). One can clearly see that the relativistic effect (mainly from the kinematic origin) makes the pion dispersion relation harder at low momenta and softer at high momenta. Furthermore, the relativistic effect at low momenta mainly comes from the nonresonant terms, i.e., the first and second terms on the RHS of Eq. (E6). If one switches off these two terms, at low momenta the results (the dash-dotted line) approach the dashed line while at high momenta they approach the dotted line. Figure 12(b) depicts the pion dispersion relation (both the pion and the Δ-hole branches) at different densities calculated with Eqs. (E5) and (E6) and $p_\mu^2\rightarrow-\mathbf{p}^2$. The short-range correlation effect is included through Eq. (125) ($p_\mu^2\rightarrow-\mathbf{p}^2$) with $g'=0.6$. As one can see from the figure, the obtained pion dispersion relation is nearly the same as that of the nonrelativistic model [16,21] except the pion branch is a little harder at high momenta. In this case one may conclude that the difference between the results of Fig. 6 and that of the nonrelativistic model mainly stems from the relativistic kinetics.

APPENDIX F

In this appendix we derive the conserved current and energy-momentum tensor.

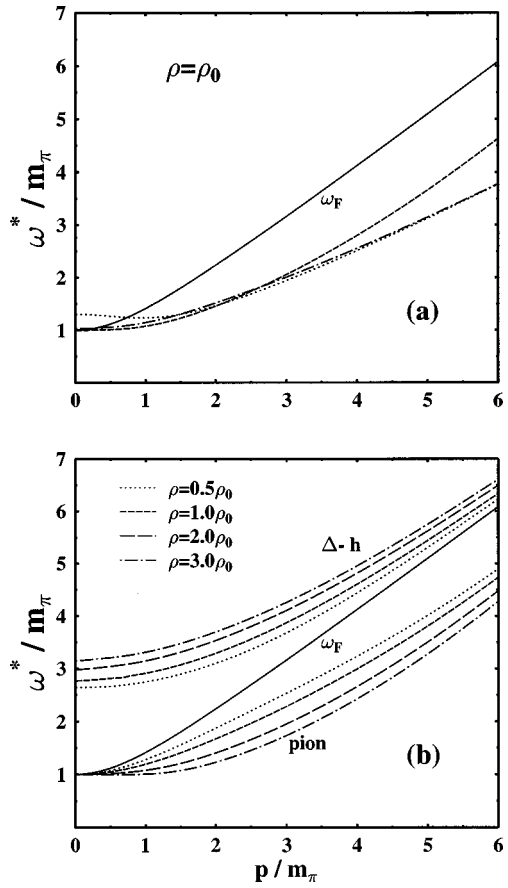

FIG. 12. (a) The pion dispersion relation (the pion branch) at normal density. Different lines correspond to the different situations as explained in text. (b) The pion dispersion relation (the pion and Δ-hole branch) at different densities. The calculations are performed with Eqs. (E5) and (E6) and $p_\mu^2 \to -\mathbf{p}^2$. The short-range correlation effect is taken into account by means of the Migdal parameter of $g'=0.6$.

(1) *Current.* Make a four-dimension integration of momentum on both sides of Eq. (62), the right-hand side (the collision term) goes to zero [77] and we have

$$\int d^4p \left\{ p^\mu \partial_\mu^x + \frac{1}{2}\partial_x^\mu \Pi_H(x)\partial_\mu^p + \frac{1}{2}\partial_x^\mu \,\mathrm{Re}\,\Pi_{\mathrm{loop}}^{--}(x,p)\partial_\mu^p - \frac{1}{2}\partial_p^\mu \,\mathrm{Re}\,\Pi_{\mathrm{loop}}^{--}(x,p)\partial_\mu^x \right\} \frac{f_\pi(\mathbf{x},\mathbf{p},\tau)}{\omega^*(p)} = 0. \tag{F1}$$

It is straightforward to find the current conservation

$$\partial_x^\mu J_\mu(x) = 0, \tag{F2}$$

with

$$J_\mu(x) = \int d^4p \left[p_\mu - \frac{1}{2}[\partial_\mu^p \,\mathrm{Re}\,\Pi_{\mathrm{loop}}^{--}(x,p)] \right] \frac{f_\pi(\mathbf{x},\mathbf{p},\tau)}{\omega^*(p)}. \tag{F3}$$

We note that each $f_\pi(\mathbf{x},\mathbf{p},\tau)$ is in principle accompanied by a δ function $\delta(p_0-\omega^*(p))$ for on-shell pions.

(2) *Energy-momentum tensor.* Multiplying p_μ on both sides of Eq. (62) and making a four-dimensional integration of the momentum, we arrive at

$$\int d^4p\, p_\mu \left\{ p_\nu \partial_x^\nu + \frac{1}{2}\partial_x^\nu \Pi_H(x)\partial_\nu^p + \frac{1}{2}\partial_x^\nu \mathrm{Re}\Pi_{\mathrm{loop}}^{--}(x,p)\partial_\nu^p - \frac{1}{2}\partial_\nu^p \mathrm{Re}\Pi_{\mathrm{loop}}^{--}(x,p)\partial_x^\nu \right\} \frac{f_\pi(\mathbf{x},\mathbf{p},\tau)}{\omega^*(p)} = 0. \tag{F4}$$

Our strategy is to extract the ∂_x^ν out of the whole equation. For the first term it is straightforward. The second term can be rewritten as

$$-g_{\mu\nu}\int d^4p \frac{f_\pi(\mathbf{x},\mathbf{p},\tau)}{2\omega^*(p)}[\partial_x^\nu \Pi_H(x)].$$

With the help of Eqs. (73) and (74), it becomes

$$\partial_x^\nu \left[g_{\mu\nu}\frac{1}{8}(g_{\sigma\pi})^2 \rho_S^2(\pi) \right].$$

The third and fourth terms can be written as

$$\begin{aligned}
&\int d^4p\, p_\mu \partial_\nu^p \left[\frac{1}{2}[\partial_x^\nu \,\mathrm{Re}\,\Pi_{\mathrm{loop}}^{--}(x,p)]\frac{f_\pi(\mathbf{x},\mathbf{p},\tau)}{\omega^*(p)} \right] - \int d^4p\, p_\mu \partial_x^\nu \left[\frac{1}{2}[\partial_\nu^p \,\mathrm{Re}\,\Pi_{\mathrm{loop}}^{--}(x,p)]\frac{f_\pi(\mathbf{x},\mathbf{p},\tau)}{\omega^*(p)} \right] \\
&= -g_{\mu\nu}\int d^4p \frac{1}{2}[\partial_x^\nu \,\mathrm{Re}\,\Pi_{\mathrm{loop}}^{--}(x,p)]\frac{f_\pi(\mathbf{x},\mathbf{p},\tau)}{\omega^*(p)} - \partial_x^\nu \int d^4p \frac{1}{2}p_\mu[\partial_\nu^p \,\mathrm{Re}\,\Pi_{\mathrm{loop}}^{--}(x,p)]\frac{f_\pi(\mathbf{x},\mathbf{p},\tau)}{\omega^*(p)} \\
&= -g_{\mu\nu}\partial_x^\nu \int d^4p \frac{1}{2}\,\mathrm{Re}\,\Pi_{\mathrm{loop}}^{--}(x,p)\frac{f_\pi(\mathbf{x},\mathbf{p},\tau)}{\omega^*(p)} + g_{\mu\nu}\int d^4p \frac{1}{2}\,\mathrm{Re}\,\Pi_{\mathrm{loop}}^{--}(x,p)\partial_x^\nu \frac{f_\pi(\mathbf{x},\mathbf{p},\tau)}{\omega^*(p)} \\
&\quad - \partial_x^\nu \int d^4p \frac{1}{2}p_\mu[\partial_\nu^p \,\mathrm{Re}\,\Pi_{\mathrm{loop}}^{--}(x,p)]\frac{f_\pi(\mathbf{x},\mathbf{p},\tau)}{\omega^*(p)}.
\end{aligned} \tag{F5}$$

The second term of the above equation turns out to be

$$
\begin{aligned}
&-\frac{1}{4}g_{\mu\nu}\int d^4p(\partial_p^\lambda p_\lambda)\,\mathrm{Re}\,\Pi_{\mathrm{loop}}^{--}(x,p)\partial_x^\nu\frac{f_\pi(\mathbf{x},\mathbf{p},\tau)}{\omega^*(p)}\\
&\quad=\frac{1}{4}g_{\mu\nu}\int d^4pp_\lambda[\partial_p^\lambda\,\mathrm{Re}\,\Pi_{\mathrm{loop}}^{--}(x,p)]\partial_x^\nu\frac{f_\pi(\mathbf{x},\mathbf{p},\tau)}{\omega^*(p)}+\frac{1}{4}g_{\mu\nu}\int d^4pp_\lambda\,\mathrm{Re}\,\Pi_{\mathrm{loop}}^{--}(x,p)\partial_p^\lambda\partial_x^\nu\frac{f_\pi(\mathbf{x},\mathbf{p},\tau)}{\omega^*(p)}\\
&\quad=\frac{1}{4}g_{\mu\nu}\int d^4pp_\lambda[\partial_p^\lambda\,\mathrm{Re}\,\Pi_{\mathrm{loop}}^{--}(x,p)]\partial_x^\nu\frac{f_\pi(\mathbf{x},\mathbf{p},\tau)}{\omega^*(p)}+\frac{1}{4}g_{\mu\nu}\int d^4pp_\lambda[\partial_x^\nu\partial_p^\lambda\,\mathrm{Re}\,\Pi_{\mathrm{loop}}^{--}(x,p)]\frac{f_\pi(\mathbf{x},\mathbf{p},\tau)}{\omega^*(p)}\\
&\quad=\partial_x^\nu\frac{1}{4}g_{\mu\nu}\int d^4pp_\lambda[\partial_p^\lambda\,\mathrm{Re}\,\Pi_{\mathrm{loop}}^{--}(x,p)]\frac{f_\pi(\mathbf{x},\mathbf{p},\tau)}{\omega^*(p)}.
\end{aligned}
\tag{F6}
$$

In the first and second equalities of Eq. (F6) we have used the fact that the terms with the double derivative acting on the same quantity can be neglected in the gradient expansion. At the end we have the energy-momentum conservation

$$
\partial_x^\nu T_{\mu\nu}(x)=0, \tag{F7}
$$

with

$$
\begin{aligned}
T_{\mu\nu}(x)=&\int d^4pp_\mu p_\nu\frac{f_\pi(\mathbf{x},\mathbf{p},\tau)}{\omega^*(p)}+g_{\mu\nu}\frac{1}{8}(g_{\sigma\pi})^2\rho_S^2(\pi)-g_{\mu\nu}\frac{1}{2}\int d^4p\,\mathrm{Re}\,\Pi_{\mathrm{loop}}^{--}(x,p)\frac{f_\pi(\mathbf{x},\mathbf{p},\tau)}{\omega^*(p)}\\
&-\frac{1}{2}\int d^4pp_\mu[\partial_\nu^p\,\mathrm{Re}\,\Pi_{\mathrm{loop}}^{--}(x,p)]\frac{f_\pi(\mathbf{x},\mathbf{p},\tau)}{\omega^*(p)}+g_{\mu\nu}\frac{1}{4}\int d^4pp_\lambda[\partial_p^\lambda\,\mathrm{Re}\,\Pi_{\mathrm{loop}}^{--}(x,p)]\frac{f_\pi(\mathbf{x},\mathbf{p},\tau)}{\omega^*(p)}.
\end{aligned}
\tag{F8}
$$

[1] M. Gyulassy and W. Greiner, Ann. Phys. (N.Y.) **109**, 485 (1977).
[2] A. B. Migdal, Rev. Mod. Phys. **50**, 107 (1978).
[3] A. Sandoval, R. Stock, H. E. Stelzer, R. E. Renfordt, J. W. Harris, J. P. Brannigan, J. V. Geaga, L. J. Rosenberg, L. S. Schroeder, and K. L. Wolf, Phys. Rev. Lett. **45**, 874 (1980).
[4] R. Stock, R. Bock, R. Brockmann, J. W. Harris, A. Sandoval, H. Ströbele, K. L. Wolf, H. G. Pugh, L. S. Schroeder, M. Maier, R. E. Renfordt, A. Dacal, and M. E. Ortiz, Phys. Rev. Lett. **49**, 1236 (1982).
[5] J. W. Harris, R. Bock, R. Brockmann, A. Sandoval, R. Stock, H. Stroebele, G. Odyniec, H. G. Pugh, L. Schroeder, R. E. Renfordt, D. Schall, D. Bangert, W. Rauch, and K. L. Wolf, Phys. Lett. **153B**, 377 (1985).
[6] O. Schwalb and the TAPS Collaboration, Phys. Lett. B **321**, 20 (1994).
[7] C. Müntz and the Kaos Collaboration, Z. Phys. A **352**, 175 (1995); **357**, 399 (1997).
[8] F. D. Berg and the TAPS Collaboration, Z. Phys. A **340**, 297 (1991).
[9] J. C. Kintner, Phys. Rev. Lett. **78**, 4165 (1997).
[10] H. Stöcker, W. Greiner, and W. Scheid, Z. Phys. A **286**, 121 (1978).
[11] P. Danielewicz, Nucl. Phys. **A314**, 465 (1979).
[12] H. Stöcker, A. A. Ogloblin, and W. Greiner, Z. Phys. A **303**, 259 (1981).
[13] W. Weise, Nucl. Phys. **A434**, 685c (1985).
[14] V. F. Dmitriev and T. Suzuki, Nucl. Phys. **A438**, 697 (1985).
[15] H.-Th. Elze, M. Gyulassy, D. Vasak, H. Heinz, H. Stöcker, and W. Greiner, Mod. Phys. Lett. A **2**, 451 (1987).
[16] L. H. Xia, C. M. Ko, L. Xiong, and J. Q. Wu, Nucl. Phys. **A485**, 721 (1988).
[17] C. M. Ko, L. H. Xia, and P. J. Siemens, Phys. Lett. B **231**, 16 (1989).
[18] G. E. Brown, V. Koch, and M. Rho, Nucl. Phys. **A535**, 701 (1991).
[19] P. Danielewicz and G. F. Bertsch, Nucl. Phys. **A533**, 712 (1991).
[20] B. A. Li and W. Bauer, Phys. Lett. B **254**, 335 (1991); Phys. Rev. C **44**, 450 (1991).
[21] W. Ehehalt, W. Cassing, A. Engel, U. Mosel, and Gy. Wolf, Phys. Lett. B **298**, 31 (1993).
[22] L. Xiong, C. M. Ko, and V. Koch, Phys. Rev. C **47**, 788 (1993).
[23] T. Herbert, K. Wehrberger, and F. Beck, Nucl. Phys. **A541**, 699 (1992).
[24] S. A. Bass, C. Hartnack, H. Stöcker, and W. Greiner, Phys. Rev. C **51**, 3343 (1995).
[25] Liang-gang Liu, Phys. Rev. C **51**, 3421 (1995).
[26] C. Fuchs, L. Sehn, E. Lehmann, J. Zipprich, and A. Fässler, Phys. Rev. C **55**, 411 (1997).
[27] C. Gale and J. Kapusta, Phys. Rev. C **35**, 2107 (1987); **38**, 2659 (1988).
[28] G. Q. Li, C. M. Ko, G. E. Brown, and H. Sorge, Nucl. Phys. **A611**, 539 (1996).
[29] C. Ernst, Diploma thesis, Frankfurt University, 1998.
[30] E. L. Bratkovskaya and W. Cassing, Nucl. Phys. **A619**, 413 (1997).
[31] G. Agakichiev and the CERES Collaboration, Phys. Rev. Lett. **75**, 1272 (1995).
[32] R. Rapp, G. Chanfray, and J. Wambach, Nucl. Phys. **A617**, 472 (1997).
[33] G. Q. Li, C. M. Ko, and G. E. Brown, Phys. Rev. Lett. **75**, 4007 (1995).

[34] W. Cassing, W. Ehehalt, and C. M. Ko, Phys. Lett. B **363**, 35 (1995).
[35] A. Wagner *et al.*, GSI scientific report, 1996, p. 56.
[36] D. Pelte and the FOPI Collaboration, Z. Phys. A **359**, 55 (1997).
[37] S. Teis, W. Cassing, M. Effenberger, A. Hombach, U. Mosel, and Gy. Wolf, Z. Phys. A **359**, 297 (1997).
[38] C. Odyniec *et al.*, LBL Report No. 24580, 1988, p. 215.
[39] J. Gosset *et al.*, Phys. Rev. Lett. **62**, 1251 (1989).
[40] T. Ericson and W. Weise, *Pions and Nuclei* (Clarendon, Oxford, 1988).
[41] C. M. Ko, Q. Li, and R. Wang, Phys. Rev. Lett. **59**, 1084 (1987); Q. Li, J. Q. Wu, and C. M. Ko, Phys. Rev. C **39**, 849 (1989).
[42] G. F. Bertsch and S. das Gupta, Phys. Rep. **160**, 189 (1988).
[43] B. Blättel, V. Koch, W. Cassing, and U. Mosel, Phys. Rev. C **38**, 1767 (1988).
[44] M. Schönhofen, M. Cubero, M. Gering, M. Sambataro, H. Feldmeier, and W. Nörenberg, Nucl. Phys. **A504**, 875 (1989); M. Schönhofen, M. Cubero, B. L. Friman, W. Nörenberg, and Gy. Wolf, *ibid.* **A572**, 112 (1994).
[45] Hongbo Zhou, Zhuxia Li, Yizhong Zhuo, and Guangjun Mao, Nucl. Phys. **A580**, 627 (1994).
[46] Shun-Jin Wang, Bao-An Li, Wolfgang Bauer, and Jorgen Randrup, Ann. Phys. (N.Y.) **209**, 251 (1991).
[47] Mao Guangjun, Li Zhuxia, Zhuo Yizhong, Han Yinlu, Yu Ziqiang, and M. Sano, Z. Phys. A **347**, 173 (1994).
[48] Guangjun Mao, Zhuxia Li, Yizhong Zhuo, Yinlu Han, and Ziqiang Yu, Phys. Rev. C **49**, 3137 (1994); Guangjun Mao, Zhuxia Li, Yizhong Zhuo, and Ziqiang Yu, Phys. Lett. B **327**, 183 (1994).
[49] Zhuxia Li, Guangjun Mao, and Yizhong Zhuo, in *Hot and Dense Nuclear Matter*, Vol. 335 of *NATO Advanced Study Institute, Series B: Physics*, edited by W. Greiner, H. Stöcker, and A. Gallmann (Plenum, New York, 1994), p. 659.
[50] Guangjun Mao, Zhuxia Li, and Yizhong Zhuo, Phys. Rev. C **53**, 2933 (1996).
[51] Guangjun Mao, Zhuxia Li, Yizhong Zhuo, and Enguang Zhao, Phys. Lett. B **378**, 5 (1996).
[52] Guangjun Mao, Zhuxia Li, Yizhong Zhuo, and Enguang Zhao, Phys. Rev. C **55**, 792 (1997).
[53] Guangjun Mao, L. Neise, H. Stöcker, W. Greiner, and Zhuxia Li, Phys. Rev. C **57**, 1938 (1998).
[54] John E. Davis and Robert J. Perry, Phys. Rev. C **43**, 1893 (1991).
[55] S. Mrówczyński and U. Heinz, Ann. Phys. (N.Y.) **229**, 1 (1994).
[56] B. D. Serot and J. D. Walecka, Adv. Nucl. Phys. **16**, 1 (1986).
[57] P. Danielewicz, Ann. Phys. (N.Y.) **152**, 239 (1984).
[58] Kuangchao Chou, Zhaobin Su, Bailin Hao, and Lu Yu, Phys. Rep. **118**, 1 (1985).
[59] H. Pilkuhn, W. Schmidt, A. D. Martin, C. Michael, F. Steiner, B. R. Martin, M. M. Nagels, and J. J. de Swart, Nucl. Phys. **B65**, 460 (1973).
[60] B. S. Zou and D. V. Bugg, Phys. Rev. D **50**, 591 (1994).
[61] J. Boguta and H. Stöcker, Phys. Lett. **120B**, 289 (1983).
[62] A. R. Bodmer, Nucl. Phys. **A526**, 703 (1991).
[63] Y. Sugahara and H. Toki, Nucl. Phys. **A579**, 557 (1994).
[64] Bernard ter Haar and Rudi Malfliet, Phys. Rev. C **36**, 1611 (1987).
[65] G. Q. Li and R. Machleidt, Phys. Rev. C **49**, 566 (1994).
[66] Song Gao, Yi-Jun Zhang, and Ru-Keng Su, Phys. Rev. C **52**, 380 (1995).
[67] V. Metag, Nucl. Phys. **A553**, 283c (1993); R. Averbeck *et al.*, GSI science report 1994, p. 80.
[68] P. A. Henning and H. Umezawa, Nucl. Phys. **A571**, 617 (1994); R. Rapp and J. Wambach, *ibid.* **A573**, 626 (1994); R. Rapp, G. Chanfray, and J. Wambach, *ibid.* **A617**, 472 (1997).
[69] David Lurié, *Particles and Fields* (J. W. Arrowsmith Ltd., Bristol, England, 1968).
[70] Wim Botermans and Rudi Malfliet, Phys. Lett. B **215**, 617 (1988); Phys. Rep. **198**, 115 (1990).
[71] G. E. Brown, E. Oset, M. Vicente Vacas, and W. Weise, Nucl. Phys. **A505**, 823 (1989).
[72] L. P. Kadanoff and G. Baym, *Quantum Statistical Mechanics* (Benjamin, New York, 1962).
[73] S. Mrówczyński and P. Danielewicz, Nucl. Phys. **B342**, 345 (1990).
[74] M. Beyer and G. Röpke, Phys. Rev. C **56**, 2636 (1997).
[75] C. J. Horowitz and B. D. Serot, Nucl. Phys. **A399**, 529 (1983).
[76] Gy. Wolf, W. Cassing, and U. Mosel, Nucl. Phys. **A545**, 139c (1992); **A552**, 549 (1993).
[77] S. R. de Groot, W. A. van Leeuwen, and Ch. G. van Weert, *Relativistic Kinetic Theory* (North-Holland, Amsterdam, 1980).
[78] H. M. Pilkuhn, *Relativistic Particle Physics* (Springer-Verlag, Berlin, 1979).
[79] Zhuxia Li, Guangjun Mao, Yizhong Zhuo, and Walter Greiner, Phys. Rev. C **56**, 1570 (1997).
[80] S. A. Moszkowski, Phys. Rev. D **9**, 1613 (1974); S. I. A. Garpman, N. K. Glendenning, and Y. J. Karant, Nucl. Phys. **A322**, 382 (1979).
[81] B. M. Waldhauser, J. Theis, J. A. Maruhn, H. Stöcker, and W. Greiner, Phys. Rev. C **36**, 1019 (1987); P. Lévai, B. Lukács, B. Waldhauser, and J. Zimányi, Phys. Lett. B **177**, 5 (1986).
[82] K. A. Brueckner, Phys. Rev. **86**, 106 (1952).
[83] A. A. Carter, J. R. Williams, D. V. Bugg, P. J. Bussey, and D. R. Dance, Nucl. Phys. **B26**, 445 (1971).
[84] Y. Kitazoe, M. Sano, H. Toki, and H. Nagamiya, Phys. Lett. **166B**, 35 (1986).
[85] Gy. Wolf, G. Batko, W. Cassing, U. Mosel, K. Niita, and M. Schäfer, Nucl. Phys. **A517**, 615 (1990).
[86] S. A. Bass, Ph.D. thesis, Frankfurt University (unpublished).
[87] Hungchong Kim, S. Schramm, and Su Houng Lee, Phys. Rev. C **56**, 1582 (1997).
[88] M. Effenberger, A. Hombach, S. Teis, and U. Mosel, Nucl. Phys. **A613**, 353 (1997).
[89] It should be mentioned that a recent experimental determination of the effective pion mass from pionic atoms gives $m_\pi^*(\rho_0)=167$ MeV [E. Friedman and A. Gal, Phys. Lett. B **432**, 235 (1998)]. Our model predicts $m_\pi^*(\rho_0)=180$ MeV. The agreement between the theoretical prediction and the empirical value might be further improved through including the short-range correlation effect self-consistently.
[90] G. Q. Li, G. E. Brown, C. Gale, and C. M. Ko, talk presented at the APCTP (Asia Pacific Center for Theoretical Physics) Workshop on Hadrons in Medium, Seoul, 1997 (unpublished), nucl-th/9712048.
[91] E. L. Bratkovskaya, W. Cassing, R. Rapp, and J. Wambach, Nucl. Phys. **A634**, 168 (1998).
[92] C. Ernst, S. A. Bass, M. Belkacem, H. Stöcker, and W. Greiner, Phys. Rev. C **58**, 447 (1998).